

**Die Expedition ARCTIC '96  
des FS "Polarstern" (ARK XII)  
mit der Arctic Climate System Study (ACSYS)**

---

**The expedition ARCTIC '96  
of RV "Polarstern" (ARK XII)  
with the Arctic Climate System Study (ACSYS)**

**Ernst Augstein and Cruise Participants**

**Ber. Polarforsch. 234 (1997)  
ISSN 0176 - 5027**



## Contents / Inhaltsverzeichnis

1.	Zusammenfassung	3
2.	Summary and Itinerary	7
3.	Research Programmes	10
3.1	Physical and Chemical Oceanography	10
3.1.1	Introduction	10
3.1.2	Methods and First Result of Temperature, Salinity and Oxygen Measurements	11
3.1.3	Nutrients	13
3.1.4	Carbonate System	14
3.1.5	Chloroflourocarbons	15
3.1.6	Tritium, Helium and $^{18}\text{O}$	15
3.1.7	Inorganic Minor Element Tracers	15
3.1.8	Volatile Halogenated Organic Compounds	16
3.1.9	Dissolved Organic Matter	17
3.1.10	Physical and Chemical Speciation of Plutonium (and Americum) in the Arctic Water Column	18
3.1.11	Acoustic Doppler Current Profiler (ADCP)	19
3.1.12	Shipborne ADCP	19
3.1.13	Optics	20
3.1.14	Ocean Moorings	21
3.2	Oceanographic / Meteorological Buoys	22
3.3	The Atmospheric Boundary Layer	23
3.4	Sea Ice Physics and Biology	27
3.4.1	Visual Ice Observations	27
3.4.2	On Ice Measurements	30
3.4.3	Laser Altimeter	30
3.4.4	Ice and Snow Thickness	30
3.4.5	Ridge Sail Profiles	32
3.4.6	Trafficability	33
3.4.7	Sea Ice Remote Sensing	35
3.4.8	Biological and Physical Sea Ice Properties	37
3.5	Marine Biology	41
3.5.1	Phyto- and Zooplankton Ecology and Vertical Particle Flux	41

3.5.2	Biomass Distribution	41
3.5.3	Taxonomy and Spatial Distribution of the Microplanktonic Community	42
3.5.4	Epipelagic Community	43
3.5.5	Meso- and Bathypelagic Communities	45
4.	Station List	47
5.	Participating Institutions	51
6.	Participants	53
7.	Ship's Crew	54

## ARCTIC '96 Cruise Report / Fahrtbericht

### 1. Zusammenfassung

Die Expedition ARCTIC '96 wurde von zwei Forschungsschiffen, der deutschen POLARSTERN und der schwedischen ODEN unter Beteiligung von Wissenschaftlern und Technikern aus Deutschland, Finnland, Großbritannien, Irland, Kanada, Norwegen, Rußland, Schweden und den Vereinigten Staaten von Amerika durchgeführt. Das gemeinsam entworfene multidisziplinäre Forschungsprogramm wurde unter Berücksichtigung der spezifischen zeitlichen und logistischen Anforderungen der einzelnen Arbeitsgruppen unter den beiden Schiffen passend aufgeteilt. Demgemäß bildeten auf der ODEN die geologischen, geophysikalischen und luftchemischen Arbeiten sowie die Eisfernerkundung das Schwergewicht, während auf der POLARSTERN vorrangig Messungen zur physikalischen, chemischen und biologischen Ozeanographie, Atmosphärenphysik und der Erforschung des Meereises vorgenommen wurden.

Die physikalischen Projekte auf der POLARSTERN dienten überwiegend der Unterstützung der Arctic Climate System Study (ACSYS) des Weltklimaforschungsprogramms, die auf die Erforschung der vorherrschenden ozeanischen, atmosphärischen, kryosphärischen und hydrologischen Prozesse der Arktisregion ausgerichtet ist. Dabei soll der Beschreibung und numerischen Modellierung der Zirkulation, Wassermassenmodifikation sowie der Transporte von Energie und Stoffen im Nordpolarmeer einschließlich seiner Randmeere besondere Aufmerksamkeit gewidmet werden. Im Hinblick auf diese Ziele wurden auf POLARSTERN Messungen durchgeführt um

- die hydrographischen Strukturen des Ozeans auf der Schnittlinie von Franz-Joseph-Land nach Severnaya Zemiya zu erfassen und den Wassermassen-austausch zwischen den flachen sibirisch-europäischen Schelfmeeren und dem tiefen Nordpolarmeer durch den St. Anna- und den Voronin-Trog abzuschätzen.
- die Ozeanzirkulation in dem Nansen- und Amundsen-Becken quantitativ zu beschreiben unter besonderer Beachtung der topographischen Einflüsse des Lomonossow Rückens und anderer Bodenstrukturen.
- die zeitlichen Variationen der Strömungen entlang des Kontinentalabhanges und über dem Lomonossow Rücken sowie der mit ihnen verknüpften Wärme- und Salztransporte festzustellen.
- den atmosphärischen Antrieb des Meereises bei verschiedenen großräumigen Luftströmungen zu bestimmen.
- statistisch signifikante Aussagen über die Dicke und die Morphologie des Meereises in verschiedenen Regionen des Nordpolarmeeres zu ermöglichen.

Neben diesen auf die ACSYS bezogenen Arbeiten wurden Beobachtungen zum Studium der Meereislebewesen, der regionalen Verteilung des Phyto- und

Zooplanktons und die Analyse bedeutsamer chemischer Prozesse in unterschiedlichen Zirkulationsästen des Nordpolarmeeres vorgenommen. Zu diesem Zweck wurden Messungen vom Schiff aus, mit Hilfe von Hubschraubern und auf dem Meereis mit verschiedenen teilweise neu entwickelten Instrumenten durchgeführt. Die physikalischen und chemischen Daten dienen unter anderem auch der Überprüfung und Verbesserung von Ozean-, Meereis- und Klimamodellen.

An Bord der POLARSTERN befanden sich 43 Seeleute, ein russischer Eislotse und 53 Wissenschaftler und Techniker aus Deutschland (29), Schweden (7), Rußland (6), USA (5), Kanada (3), Finnland (1), Irland (1) und Großbritannien (1). Das Meßprogramm wurde von multinationalen Arbeitsgruppen durchgeführt, die später auch die Datenaufbereitung und wissenschaftliche Bewertung der Ergebnisse gemeinsam vornehmen werden. Die Zusammenarbeit zwischen der ODEN und der POLARSTERN während der Expedition bezog sich im wesentlichen auf logistische Unterstützung. Während zweier Treffen auf See fand ein Personalaustausch statt und es wurden Instrumente und Treibstoff umgeladen. Zur gegenseitigen Information über den Arbeitsablauf, die Wetter- und Eisverhältnisse wurden täglich Funkgespräche zwischen den wissenschaftlichen Leitern und den Kapitänen beider Schiffe geführt.

POLARSTERN lief am Freitag, den 12. Juli 1996 aus Bremerhaven aus und erreichte nach einer ruhigen Seereise am 19. Juli den russischen Hafen Murmansk, wo sich 7 russische und ein finnischer Wissenschaftler sowie 2 Eislotsen einschifften. Repräsentanten der Behörden und wissenschaftlichen Einrichtungen der Stadt besuchten am Nachmittag des 19. Juli das Schiff anlässlich eines kleinen Empfangs. Am 20. Juli verließ POLARSTERN Murmansk mit dem Ziel Karasee. Außerhalb der 12-Meilenzone wurde noch einmal Treibstoff von einem Tankschiff übernommen, um für den langen Aufenthalt im eisbedeckten Nordpolarmeer gut gerüstet zu sein. Die Packeisgrenze wurde am 23. Juli bei 78°N überquert, einen halben Tag vor dem ersten Treffen mit der ODEN, die bereits einige Tage in der Barentssee Messungen durchgeführt hatte. Während die Schiffe für einige Stunden zusammen drifteten wechselten ein Eislotse und ein Wissenschaftler von der POLARSTERN zur ODEN während der für beide Schiffe zuständige russische Beobachter in umgekehrter Richtung zur POLARSTERN überstieg. Ferner wurden der ODEN einige aus Deutschland mitgeführte Geräte übergeben.

Nach einigen Stunden Fahrt im Konvoi trennten sich die Schiffe am 24. Juli 1996, indem die ODEN ihren nordwärtigen Kurs zum Lomonossow-Rücken fortsetzte und POLARSTERN nach Osten steuerte, um das Meßprogramm mit einem zonalen hydrographischen Schnitt zwischen Franz-Joseph-Land und Severnaya Zemlya aufzunehmen (Figure 1). Dort wurden mit einer CTD (conductivity, temperature, depth) - Sonde, einem Wasserschöpfsystem und einem ADCP (acoustic doppler current profiler) der thermohaline Aufbau und mit Einschränkungen das Strömungsfeld auf einer Schnittfläche durch den St. Anna- und Voronin-Trog in relativ dichten Abständen erfaßt. Ferner wurden Wasserproben zur Bestimmung ozeanischer Spurenstoffe, radioaktiver Isotope und verschiedener Nährstoffe geschöpft sowie Planktonnetzfüge vorgenommen. Längere Meßstationen wurden - wie während der gesamten Reise im Eis - für umfangreiche Meereisbeprobungen genutzt, um an Bord oder später in den Heimatlabors physikalische, chemische und

biologische Analysen durchzuführen. Insbesondere konnten auf längeren Traversen über große Schollen mit einem neuen Meßsystem statistisch signifikante Eisdickenverteilungen registriert werden und Eisrücken detailliert vermessen werden. Schließlich dienten die von einem Hubschrauber getragene Turbulenzsonde HELIPOD und ein am Bugkran befestigter mit 5 Turbulenzsonden ausgerüsteter Profilmast zur Erfassung der vertikalen turbulenten Impuls-, Wärme- und Wasserdampftransporte. Hubschrauberflüge in verschiedenen Höhen konnten auch zur Bestimmung von Vertikalprofilen der turbulenten Flüsse und deren spektralen Verteilung bis zum Oberrand der atmosphärischen Grenzschicht genutzt werden.

Auf dem Wege nach Severnaya-Zemlya nahm die Eiskonzentration ständig zu und behinderte schließlich das Fortkommen des Schiffes so stark, daß POLARSTERN etwa 30 sm nach Norden ausweichen mußte, um den östlichen Kurs über die Tröge am 1. August 1996 bei 82°N / 90°E vollenden zu können. Nach Ausbringen der ersten automatischen meteorologischen Driftboje wurden zunächst der Kontinentalabhang und dann das Nansen Becken, der Mittelozeanische Rücken und das Amundsen Becken in nordöstlicher Richtung überquert. Dabei wurde das auf der Zonaltraverse begonnene Meßprogramm im wesentlichen in gleichartiger Weise fortgesetzt. Auf dem Weg nach Norden nahm die Eiskonzentration unerwartet deutlich ab, so daß POLARSTERN auf den Fahrtstrecken zwischen den ozeanographischen Stationen in breiten Rinnen bisweilen Geschwindigkeiten bis zu 12 kn erreichte. Dadurch wurden nicht nur die Zeitverluste des ersten Abschnittes schnell aufgeholt sondern auch eine Erweiterung des Meßprogramms vor allem an den Flanken der Tiefseerücken ermöglicht. Dabei wurde u. a. gefunden, daß der Mittelozeanische Rücken zwischen dem Nansen- und Amundsen-Becken zumindest auf der POLARSTERN-Route in den Echolotmessungen - im Gegensatz zu der uns verfügbaren Seekarte - nicht in Erscheinung trat.

Wegen der günstigen Eisverhältnisse erreichte POLARSTERN die Bohrposition der ODEN auf dem Lomonossow-Rücken drei Tage früher als geplant, so daß die zweite Begegnung beider Schiffe auf den 11./12. August vorverlegt wurde. Aufgrund der besonders günstigen Eislage einigten sich Wissenschaftler und Kapitäne darauf, die Aufnahme von drei Verankerungen am Nordrand der Laptev-See der POLARSTERN allein zu überlassen und die Fahrtroute der ODEN durch Verlagerung des Arbeitsgebiets nach Norden abzuändern. Zur Vermeidung von Treibstoffengpässen wurde Schiffsdiesel von der ODEN zur POLARSTERN und Hubschraubertreibstoff in umgekehrter Richtung transferiert. Der russische Beobachter nutzte das Treffen, um wieder auf die ODEN zurückzukehren, nachdem er einen russischen Wissenschaftler beauftragt hatte, die Beobachterfunktion auf POLARSTERN zu übernehmen. POLARSTERN setzte am 12. August den hydrographischen Schnitt vom Amundsen-Becken über den Lomonossow-Rücken fort und erreichte am 15. August das Makarov-Becken.

Die anschließende Marschfahrt nach Süden war wieder durch breite Rinnen begünstigt, so daß die gewonnene Zeit für ein erweitertes Meßprogramm auf der südlicheren Traverse über den Lomonossow-Rücken genutzt werden konnte. Im Amundsen-Becken wurde ein Meßnetz von meteorologischen und ozeanographischen automatischen Driftstationen auf dem Meereis ausgelegt, das über eine längere Zeit den atmosphärischen Antrieb und die ozeanischen Größen

in der oberen Wassersäule im Zentrum des Transpolaren Eisdriftstroms messen soll. Auf der Strecke zu den drei Verankerungen in der Umgebung des Kontinentalhanges und des südlichen Lomonossow-Rückens verdichtete sich die Eiskonzentration so stark, daß die hydrographischen Messungen im nördlichen Verankerungsgebiet sogar teilweise reduziert werden mußten. Trotz der ungünstigen Eisbedingungen gelang es, alle drei Verankerungssysteme in verhältnismäßig kurzer Zeit sicher zu bergen. Dieser Erfolg beruht zum einen auf der guten technischen Konzeption der Verankerungen und zum anderen auf dem geschickten Handeln der erfahrenen Schiffsführung und der verantwortlichen Wissenschaftler und Techniker. Der Zeitgewinn beim Bergen der Verankerungen ging zumindest in Teilen durch weiter anhaltende Fahrtverzögerungen im Preßeis wieder verloren. Neben kürzeren Zwangstillständen blieb POLARSTERN einmal 14 Stunden zwischen zusammengepreßten Schollen stecken.

Glücklicherweise war die Region gerade zu dieser Zeit wolkenarm, so daß den an Bord empfangenen Satellitenbildern nützliche Informationen über die Eisverteilung entnommen werden konnten. Danach hatten sich um 100 km lange Rinnen in Fahrtrichtung des Schiffes gebildet, die ein leichtes Vorankommen durch das im übrigen stark gepreßte Eis versprachen. Hubschraubererkundungsflüge bestätigten diesen Befund, so daß POLARSTERN nach zunächst aufwendigem Rammen innerhalb von zwei Tagen die Eisrandzone erreichen konnte. Hier stand wieder ausreichend Zeit für umfassende Messungen aller Disziplinen zur Verfügung. Insbesondere wurden die biologischen Beprobungen verdichtet und die Untersuchungen zur atmosphärischen Grenzschichtturbulenz ausgedehnt.

Nach Abschluß des gesamten Meßprogramms am 5. September 1996 verließ POLARSTERN das Meereis und lief in der nahezu eisfreien Laptevsee westwärts in Richtung Vilkitskystraße. Dort wurde auf einer kleinen Insel ein vor einem Jahr angelegtes Meßfeld auf dem Festeis mit einem Hubschrauber besucht, um Informationen über Schmelz- und Gefrierprozesse zu gewinnen.

Der Weg durch die Vilkitskystraße, die Karasee und die Barentssee bis nach Murmansk war in diesem Jahr eisfrei und erlaubte wiederum einen Zeitgewinn, der einer wünschenswerten Verlängerung der Umrüstzeit des Schiffes in Bremerhaven zugute kam. Während eines kurzen Hafenaufenthaltes in Murmansk am 15./16. September verließen ein finnischer und sechs russische Wissenschaftler sowie der Eislotse das Schiff, das dann die Reise durch die Barentssee, die Norwegische See und die Nordsee heimwärts fortsetzte. Am 23. September lief POLARSTERN in Bremerhaven ein, wo sich im Laufe des Tages alle Wissenschaftler und Techniker ausschiffen.

## 2. Summary and Itinerary

The multinational expedition ARCTIC '96 was carried out jointly by two ships, the German RV POLARSTERN and the Swedish RV ODEN. The research programme was developed by scientists from British, Canadian, Finish, German, Irish, Norwegian, Russian, Swedish and US American research institutions and universities. The multidisciplinary field programme was shared between the two ships on the basis of their specific technical capabilities. Thus, the work on the ODEN concentrated on geology, geophysics, air chemistry and sea ice remote sensing while the investigations on POLARSTERN were devoted to physical, chemical and biological oceanography, sea ice physics and biology as well as to the atmospheric boundary layer.

The physical programme on POLARSTERN was primarily designed to foster the *Arctic Climate System Study* (ACSYS) in the framework of the *World Climate Research Programme* (WCRP). Investigations during the recent years have provided substantial evidence that the Arctic Ocean and the adjacent shelf seas play a significant role in the thermohaline oceanic circulation and may therefore have a distinct influence on global climate. Consequently the main ACSYS goals are concerned with studies of the governing oceanic, atmospheric and hydrological processes in the entire Arctic region. Among those the description and modelling of the circulation, the water mass modification as well as the energy and matter transports in the Arctic Ocean are of high importance. On POLARSTERN measurements were conducted in this respect to

- specify hydrographic structures on the transect from Franz Joseph Land to Severnaya Zemlya which will enable one to determine the water mass exchanges between the shelf seas and the deep Arctic basins via the St. Anna and Voronin Troughs ,
- describe the circulation within the Nansen and Amundsen Basins as well as to detect the topographic influence of the Lomonosov Ridge on the water mass spreading across the basins,
- observe the time variations of the currents, the heat and the salt transports along the continental slope and across the ridge,
- determine the atmospheric forcing on sea ice under different large scale atmospheric flow conditions
- provide information on the thickness and surface morphology of sea ice in various regions of the Arctic Ocean.

In addition to these ACSYS related topics measurements were carried out to study the sea ice biota, to describe the lateral distribution of phytoplankton and zooplankton and to identify the governing chemical processes in the water columns of different circulation branches. For these purposes measurements were made from the ship, with the aid of helicopters and from ice floes with a series of instruments some of which have been newly developed. The physical and chemical data will, among others, serve to test and to improve present and future ocean, sea ice and climate models.

On POLARSTERN 43 crew, 1 *Russian* ice pilot and 53 scientists and technicians from *Germany* (29), *Sweden* (7), *Russia* (6), *USA* (5), *Canada* (3), *Finland* (1), *Ireland* (1) and the *United Kingdom* (1) participated in the cruise. The measurements were carried out by multinational subgroups and the processing and scientific analysis of the data will also be done jointly by members of the participating institutions in the near future. The cooperation between the ODEN and the POLARSTERN during the expedition was mainly restricted to logistic matters. During two rendezvous at sea personnel, scientific gear and fuel were exchanged.

Daily radio conferences were held for mutual information on the current activities on both ships as well as on weather and ice conditions.

POLARSTERN departed from *Bremerhaven* on Friday, 12 July 1996 and she arrived after a smooth voyage on 19 July in *Murmansk, Russia*. Here 7 *Russian* and 1 *Finish* scientists and 2 ice pilots embarked. Local representatives visited the ship during the afternoon of the same day in the framework of a cocktail reception. POLARSTERN left port again on 20 July for the Kara Sea. When she had passed the *Russian* territorial waters she met a small tanker at sea to top up her fuel tanks in final preparation for the long voyage into the ice covered Arctic Ocean. The pack ice was encountered on 23 July at about 78°N in the Barents Sea half a day before the first rendezvous with the *Swedish* partnership ODEN. During this meeting 1 scientist and 1 ice pilot as well as some instruments were transferred from POLARSTERN to ODEN and the *Russian* observer who was in charge for both ships moved to POLARSTERN to stay there for the next 3 weeks.

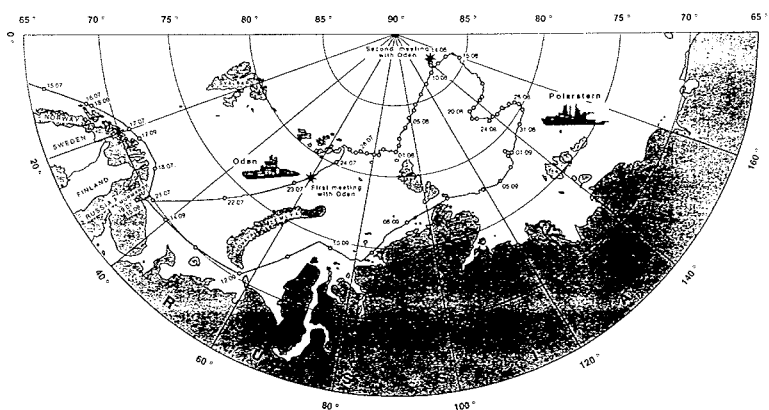


Figure 1: Cruise track of RV POLARSTERN during ARCTIC '96

The two ships separated on 24 July when POLARSTERN commenced the first hydrographic section across the St. Anna and Voronin Troughs as shown in Fig. 1 and ODEN continued her northward course towards the Lomonosov Ridge. Hydrographic vertical profiles were measured with the aid of a CTD (conductivity, temperature, depth) sonde, rosette water samplers and occasionally an acoustic doppler current profiler (ADCP). The dense hydrographic network on all transects included at various stations also biological net hauls, measurements on ice floes and atmospheric turbulence investigations. For the latter a new vertically pointing mast with acoustic anemometers and thermometers was attached to the bow crane. Furthermore, a sophisticated device, the HELIPOD which was suspended at a 15 m long cable below a helicopter to measure turbulent fluxes along specific flight tracks at various heights.

On the way from Franz Joseph Land to Severnaya Zemlya the ship's motion was increasingly slowed down towards the east by highly concentrated and partly compressed sea ice. Finally POLARSTERN had to make a 30 nm side step to the north to be able to finalise the full section across both troughs on 1 August 1996. On the eastern side of the transect the first meteorological automatic surface buoy was deployed on an ice floe. At about 82°N / 90°E POLARSTERN set course first towards north to cross the continental slope and afterwards to the northeast for a

long transect from the Kara Sea via the Nansen Basin, the Mid Oceanic Ridge, the Amundsen Basin, the Lomonosov Ridge into the Makarov Basin. The farther the ship got north the more favourable the ice conditions became. Leads grew wider and longer so that the ship could sometimes speed up to 12 knots between stations. Since our planning was based on a mean speed of 3 kn within the ice time was gained for extended measurements along the route. To our surprise the Mid Oceanic Ridge (Gakkel Ridge) was merely obvious in the echo soundings so that no orographic boundary separates the Nansen and the Amundsen Basins at least on POLARSTERN's track line. Because of the relatively fast motion of the ship we approached the ODEN at the envisaged drilling site 3 days earlier than anticipated. Thus, the second rendezvous was arranged for the 11 / 12 August 1996 over the Lomonosov Ridge. The main purpose of the meeting was to transfer ship's diesel from the ODEN to the POLARSTERN and helicopter fuel into the reverse direction. Furthermore, the *Russian* observer returned to the ODEN. During a planning meeting of the chief scientists and the masters of both ships it was concluded that according to this year's ice conditions POLARSTERN would try to retrieve three ocean moorings at the continental slope of the Laptev Sea without the assistance of ODEN. On the basis of this decision ODEN modified her plans for the research work and for her way home. POLARSTERN continued the interrupted hydrographic section and reached the Makarov Basin on 15 August 1996.

On the transit voyage to the next section across the Lomonosov Ridge the ship hit again many leads so that a significant amount of time could be saved for more measurements along the transect. An array of automatic meteorological and oceanographic surface buoys was deployed in the central Amundsen Basin. The latter provide atmospheric surface data and conduct also measurements of the temperature, salinity and currents in the upper 200 m of the water column.

During the transit to the most northerly mooring location the ice concentration increased considerably and POLARSTERN's speed was remarkably reduced. In spite of the dense ice cover the mooring could be recovered rather rapidly on 23 August due to its accurate positioning system and to the careful manoeuvring of the ship by her experienced personnel. The ship steamed then first 30 nm to the west to commence the southern zonal section across the Lomonosov Ridge. Due to compressed ice this task was rather cumbersome and finally two of the planned stations had to be skipt since helicopter reconnaissance flights made it obvious that the entire passage to the second mooring had to be made through a compact sea ice cover. POLARSTERN arrived at the second mooring position on 29 August. Fortunately there were some small patches of open water at and near the location of the mooring so that the retrieval could be managed again within a few hours time. During the completion of the meridional section across the mooring POLARSTERN had to overcome the severest ice conditions of the entire expedition and she was once trapped for 14 hours by compressed ice floes.

During the transit to the third mooring cloud free satellite images of our wider area could be received on the ship showing long and broad leads pointing from the actual ship's position towards the location of the last mooring. These indications were confirmed by helicopter flights so that the 180 nm distance could be traversed in less than two days. Since a low ice concentration prevailed over the mooring a fast and easy recovery was possible and again more time could be made available for observations and samplings. This opportunity was used on the one hand to collect additional biological material and on the other hand to extend the atmospheric boundary layer investigations in the marginal ice zone. When all measurements were completed the observational programme on POLARSTERN was terminated on 5 September 1996.

At midnight of the same day the ice edge was crossed and the homeward journey started through almost ice free waters of the Laptev Sea. The last scientific mission was carried out by a helicopter to revisit an experimental site on the fast ice of a

Because of generally stern winds in the Kara and Barents Seas the ship could move with reduced power to the port of *Murmansk* to save fuel and to avoid refuelling prior to the arrival in Bremerhaven. During the port call in Murmansk on 15 / 16 September 6 *Russian* scientists one *Finish* colleague as well as the *Russian* ice pilot disembarked. POLARSTERN arrived at her home port *Bremerhaven* on 23 September to terminate her ARCTIC '96 cruise.

### 3. Research Programmes

#### 3.1 Physical and Chemical Oceanography

(AWI, IfMH, IfMK, IUH, AARI, GU, BIO, UW, ESR, SIO, LDEO, UCD)\*

##### 3.1.1 Introduction

Waters modified in the Arctic Ocean influence the thermohaline circulation of the Atlantic Ocean and thereby also of the global ocean. As the modification of waters in the Arctic is largely controlled by shelf processes, characteristics of the inflow from the shelves are of similar importance as of the flow of different branches along the continental slope and along oceanic ridges. Our measurements are thus carried out to better comprehend the circulation pattern, flow rates and water mass modification in the *Eurasian* part of the Arctic Ocean.

Atlantic water enters the Arctic Ocean through Fram Strait and through the Barents and Kara Seas. Both branches merge over the continental slope in the eastern Nansen Basin. The Atlantic water passing through the Barents and Kara Seas is considerably modified by air-sea interaction processes and by inflow of river water. Consequently this water is colder and less saline when it meets the Fram Strait Branch of Atlantic water in the Nansen Basin so that a distinct front separates these two water masses. Various substances originating from the atmosphere and from river input or resulting from shelf specific biological processes enable us to trace the flow path of the Barents Sea Branch Water throughout the Arctic Ocean and to determine its flow rate.

From previous cruises it was concluded that both of the above mentioned branches partly recirculate in the Nansen and Amundsen Basins and partly enter the Canadian Basin across the southern Lomonosov Ridge. Deep waters may also be exchanged between the Amundsen and Makarov Basin intermittently through trenches of the Lomonosov Ridge.

Earlier measurements have already shown highly structured vertical layers which are frequently characterized by inversions of the temperature and the salinity. Some of these layers can be identified over large (basin wide) distances. The inversions are believed to result from interleaving of different water masses at frontal zones. Finally double-diffusion processes may to a certain extent alter the vertical temperature and salinity distribution of the layered structures.

The specific oceanographic goals during this cruise were to

- accomplish a hydrographic vertical section across the St. Anna and the Voronin Throughs to examine the water mass characteristics of the inflow from the Barents and Kara Seas into the Nansen Basin

\* see Chapter 5 for explanation of contributing institutions

- qualitatively and quantitatively describe the circulation in the Nansen, Amundsen and Makarov Basins as well as the exchanges of intermediate and deep waters between the different basins
- investigate the fate of shelf water within the deep basins
- determine the gas exchange (oxygen and carbon dioxide) between the partly ice covered Arctic Ocean and the atmosphere
- study processes influencing the heat, salt and momentum fluxes in the surface layer and across the halocline
- determine the optical properties of the Arctic sea water in summer conditions

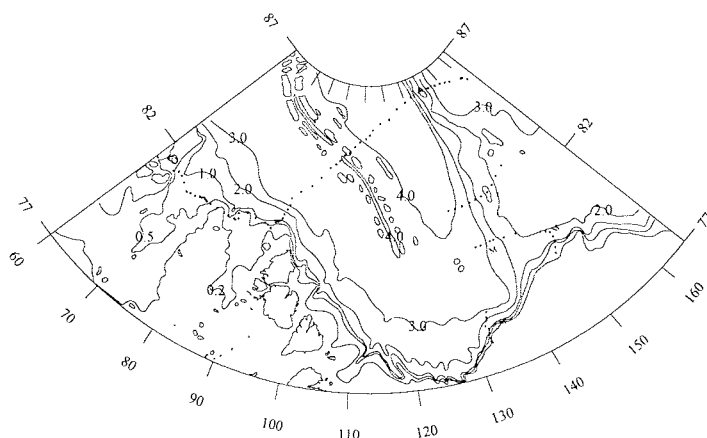


Figure 2: Dots mark all hydrographic stations and the M symbols indicate the positions of the three moorings

All observations were made on transects (Fig. 2) along the Kara Sea shelf break crossing the St. Anna and Voronin Troughs, across the Nansen and Amundsen Basins into the Makarov Basin, across the Lomonosov Ridge and across the continental slope of Laptev Sea and the East Siberian Sea. The station spacing ranged between 5 km and 30 km. CTD/rosette casts were made on all stations.

### 3.1.2 Methods and First Results of Temperature, Salinity and Oxygen Measurements

Vertical profiles of temperature and conductivity were measured with a modified *Neil Brown Mark III b* CTD system combined with a 36-bottle rosette sampler, both from the *Scripps Institution of Oceanography*. The CTD was also equipped with two platinum resistance thermometers to control the stability of its temperature sensor. The temperature and pressure gauges of the CTD were calibrated before and after the cruise. Salinity values derived from the CTD measurements were calibrated with the aid of water samples which were analyzed on board with a *Guildline Autosal 8400 B* salinometer.

The sampling and measurement of dissolved oxygen were carried out according to the WOCE protocol. Analyses of oxygen were performed by a modified *Winkler* titration procedure. The titrator has a precision of about  $\pm 0.05 \mu\text{M/kg}$  under laboratory conditions but due to sampling errors at sea the relative accuracy lies at

+/- 0.2  $\mu\text{M}/\text{kg}$ . The absolute accuracy which accounts e.g. for the systematic error caused by the natural iodate in seawater is estimated to range at 1 to 2  $\mu\text{M}/\text{kg}$ . Examples of the distributions of salinity and dissolved oxygen across the Nansen and Amundsen Basins and the Lomonosov Ridge are shown in Fig. 3 and 4, respectively.

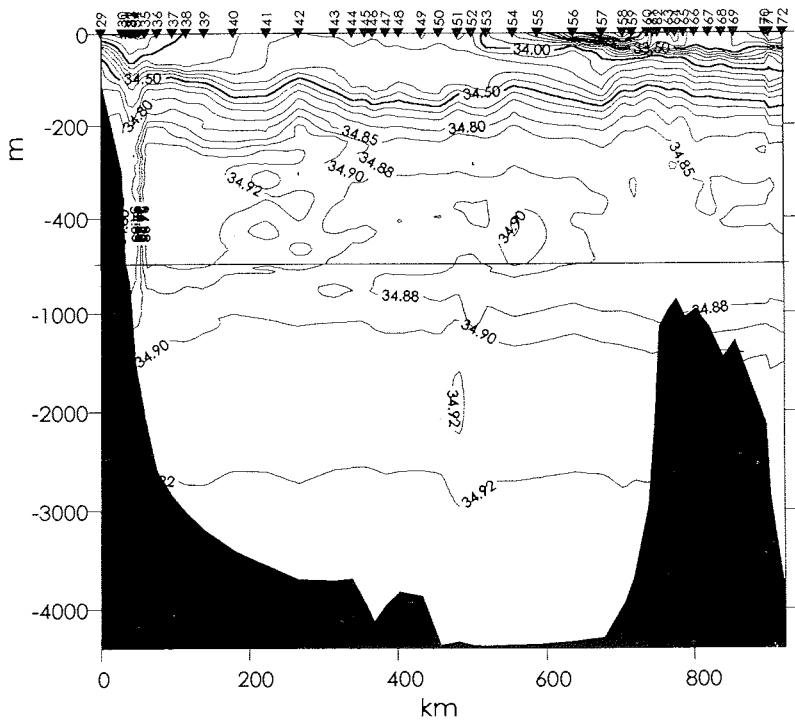


Figure 3: Salinity distribution on the section from the continental slope of the Kara Sea to the Makarov Basin

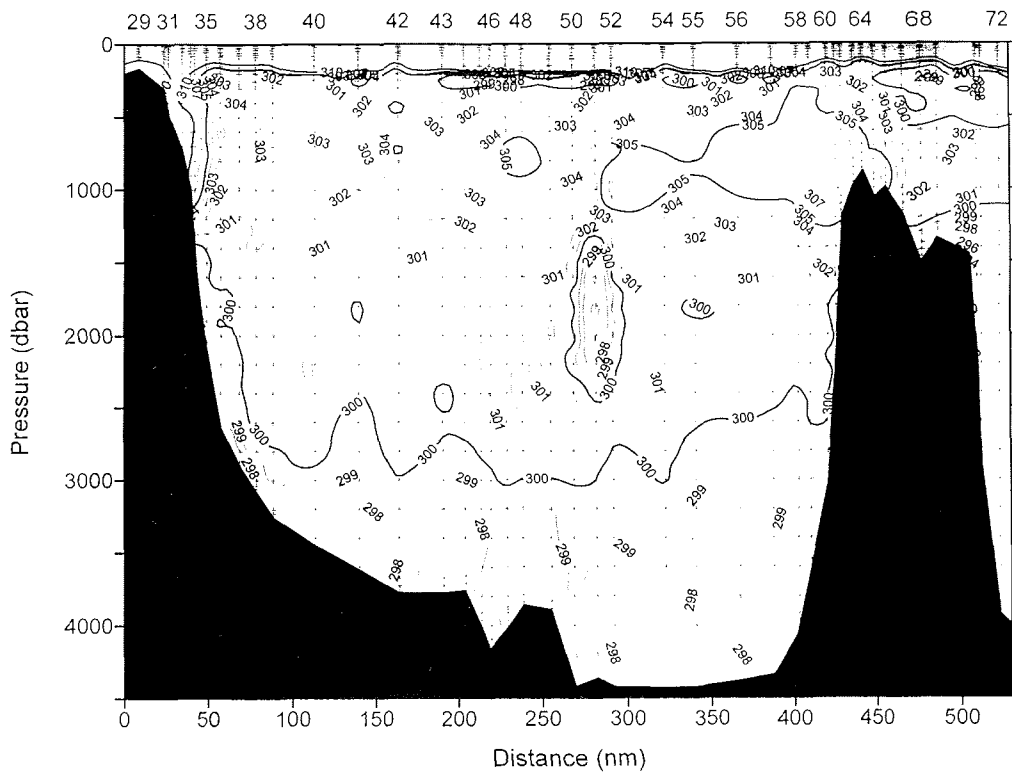


Figure 4: Same section as Fig. 3 for dissolved oxygen

### 3.1.3 Nutrients

In the Arctic Ocean nutrient concentrations provide a valuable tool to trace water masses and to detect transport and mixing mechanisms. By this means Pacific water with high silicate concentration which flows through Bering Strait can be traced via the Chukchi-East Siberian Sea to Fram Strait and the Greenland Sea. Silicate concentrations in deeper water were used to determine large scale circulation patterns and they have provided convincing evidence that the shelf-slope plume contributes to the formation of deep water.

Silicate, phosphate and total nitrate (nitrite plus nitrate), were analysed from all sampling depths at all stations. The samples were drawn in 30 ml plastic bottles, refrigerated and analysed normally within 36 hours after collection. Analyses were carried out with an *AutoAnalyzer* by standard procedures.

### 3.1.4 Carbonate System

The carbonate system was determined by analysing the rosette water samples for Total Dissolved Inorganic Carbon ( $C_T$ ), Total Alkalinity ( $A_T$ ) and pH. They are defined as

$$C_T = [\text{CO}_2] + [\text{H}_2\text{CO}_3] + [\text{HCO}_3^-] + [\text{CO}_3^{2-}]$$

$$A_T \text{ }^a [\text{HCO}_3^-] + 2[\text{CO}_3^{2-}] + [\text{B}(\text{OH})_4^-]$$

$$\text{pH} = -\log [\text{H}^+]$$

Hence, any of the carbonate species can be calculated from two of these parameters.  $C_T$  was determined by the standard coulometric technique,  $A_T$  by potentiometric titration and pH by a multi-wavelength spectrophotometric technique. Both  $A_T$  and  $C_T$  are largely correlated with salinity but some biogeochemical processes will shift their concentration.  $A_T$  is mainly affected by formation and dissolution of metal carbonates, while  $C_T$  also is affected by air-sea exchange of  $\text{CO}_2$  and by photosynthesis and microbial decay of organic matter. Like  $C_T$ , pH is affected by all of these processes. In the Arctic Ocean  $A_T$  and  $C_T$  are useful tracers of runoff, as this contains high concentration of  $\text{HCO}_3^-$  as a combined result of decay of organic matter and dissolution of metal carbonates.

The motivation for determining the carbonate system during Arctic '96 was; (i) to study shelf - deep basin interaction by using signals caused by biogenic processes on the shelves, (ii) to investigate how the runoff is spread out into the central Arctic Ocean from the Kara and Laptev Seas and (iii) to estimate the air -sea exchange of  $\text{CO}_2$  in ice covered regions.

Samples from about 75 % of the stations occupied during the cruise were analysed for all three parameters. An example of the runoff signal being stronger in the top 100 m over the Lomonosov Ridge (Stn 70) compared to the Nansen Basin (Stn 36) is shown in Fig. 5.

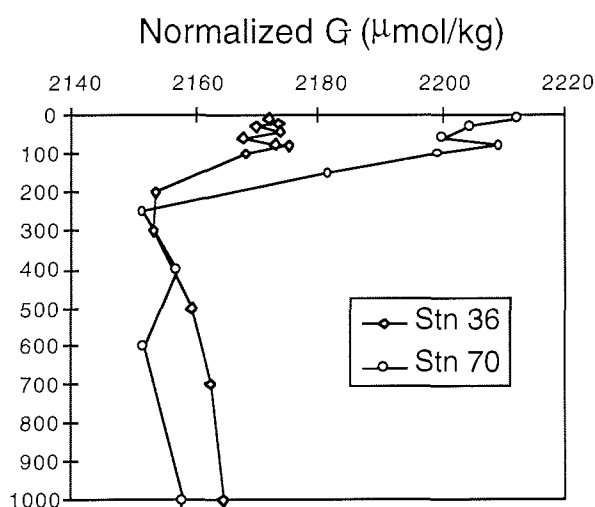


Figure 5: Depth profiles of total dissolved inorganic carbon, normalized to a salinity of 35, for stations 36 (Nansen Basin) and 70 (Lomonosov Ridge).

### 3.1.5 Chloroflourocarbons

Chloroflourocarbons measured during this expedition, CFC-11, CFC-12, CFC-113 and carbon tetrachloride (CCL<sub>4</sub>) are anthropogenic compounds the concentration of which has been increasing in the atmosphere, and hence in ocean surface waters, beginning with CCL<sub>4</sub> early in this century, CFC-11 and CFC-12 in mid-century and CFC-113 in recent decades. CFC-11 and CFC-12 are believed to be highly stable in the marine environment. CCL<sub>4</sub> is thought to be stable in cold waters below 10°C but does hydrolyze in warm waters. In the ocean these compounds help to estimate exchange rates of water and to trace water masses by distinguishing "older" water from "younger" water.

CFC measurements were made in samples from almost all stations shown in Figure 2 and from all depths. Samples were drawn in 100 ml syringes and analysed within 24 hours after sampling. Analyses were done by members of the *Institut für Meereskunde, Kiel* (IfMK) and of the *Bedford Institute of Oceanography* (BIO). Both groups used purge-and-trap systems, one measuring CFC-11 and CFC-12 (IfMK) and the other (BIO) measuring all four compounds. More than 600 of the samples were analysed. Intercalibration between the two systems resulted in sufficient agreement for CFC-12, while a ten per cent difference in CFC-11 values needs still to be explained.

### 3.1.6 Tritium, Helium and <sup>18</sup>O

Transient tracers such as Tritium/<sup>3</sup>He and stable isotopes like <sup>18</sup>O provide information on circulation and residence times of water masses. Tritium decays with a half life time of 12.43 years into stable <sup>3</sup>He. Thus, the ratio Tritium/<sup>3</sup>He can be used to determine the last time at which a water molecule has been in contact with the atmosphere. The stable isotope <sup>18</sup>O, in combination with salinity, is well suited to separate river water and sea ice meltwater fractions within the Arctic Ocean. High latitude river runoff is marked by low <sup>18</sup>O/<sup>16</sup>O values, whereas in sea ice this ratio is primarily determined by the generally higher value of the freezing sea water.

Members of the *Lamont-Doherty Earth Observatory of the Columbia University* (LDEO) and of the *Institut für Umweltphysik der Universität Heidelberg* (IUP) have collected over 800 Tritium, Helium and <sup>18</sup>O samples. The water was stored in 40 ml pinched-off copper tubes, 1 liter glass bottles and 50 ml glass bottles. The samples will be analysed at LDEO and IUP both using fully automated isotope mass spectrometers. Precision of ±0.2% for the <sup>3</sup>He/<sup>4</sup>He ratio and of ±2% for Tritium are routinely achieved.

The stable isotope ratio of <sup>18</sup>O/<sup>16</sup>O will be obtained to an accuracy of ±0.02 to 0.03 ‰.

### 3.1.7 Inorganic Minor Element Tracers

At all stations samples were taken for the *Oregon State University* to determine inorganic minor element tracers such as Rb, Cs, Ba, Sr, Li, B, F, I, Cd and isotopes of Sr and Li. Results of these analyses will be used to trace river waters along their paths in the Arctic Ocean.

### 3.1.8 Volatile Halogenated Organic Compounds

Volatile halogenated compounds are ubiquitous trace constituents of the oceans and the atmosphere. Among others halogens have the ability to affect the atmospheric ozone budget.

Bromine is found most often in compounds originating from the ocean although the bromide concentration is much lower than that of chloride in sea water. Besides of brominated substances, chlorinated and iodinated ones are also present in the oceans. But no reliable estimates are actually available on the strength of the oceanic source. Organo-chlorine compounds in the marine environment are primarily attributed to human activities (pesticides, anti-freezing agents etc.), but in addition both, macroalgae and microalgae produce chlorinated compounds such as chloroform, trichlorethylene and perchlorethylene which are emitted from the ocean into the atmosphere, where they participate in various chemical reactions. Iodinated compounds have relatively short lifetimes in the troposphere, whereas chlorinated and brominated ones may even reach the stratosphere. During this cruise the distribution of halocarbons in the water column, the formation of halocarbons by pelagic and ice-living organisms and the flux of halocarbons across the air-sea interface were investigated.

For these purposes sea water samples were collected from the rosette sampler on most of the ship's transects. Water was drawn in 100 ml glass syringes. The compounds were pre-concentrated with a purge and trap system prior to analysis with capillary gas chromatography. Due to the analysis time of 28 minutes samples could be taken from only 12 different depths. To avoid contamination of the purge and trap system with micro-organisms, all samples were filtered through a GFC filter prior to analysis. The formation of naturally produced halocarbons by different sized micro-organisms, were studied. Surface water was filtered through a unit with 5 different sized filters: 1000, 150, 12, 2 and 0.4  $\mu\text{m}$ . Each fraction contained 250 ml of water. After the filtration of approximately 25 l of water, during a period of 4 hours, the water from the different compartments was put in 60 ml glass bottles. Care was taken to avoid any headspace volume in order to minimise losses of the compounds to air. The glass bottles were put into a refrigerator, with a mean temperature of 0°C, and a light intensity of approximately 20 - 40  $\mu\text{mol photons m}^{-2} \text{ s}^{-1}$ . The formation of halocarbons was measured after 6 to 60 hours after sampling. Prior to injection, the water was filtered through a GFC filter, and the chlorophyll content was measured by standard procedures.

The lower most 20 cm of icecores were collected at 16 stations in order to determine the formation of halocarbons by ice-living organisms. 10 cm pieces of ice were put into air tight glass jars, which were also put into the refrigerator. Air samples were collected at different time intervals. Fluxes of the compounds across the air-sea interface were derived with the additional aid of the air samples.

We found the mean surface concentrations of the biogenic halocarbons to be relatively low during the entire cruise. Bromoform is generally produced by macroalgae in rather high quantities and to a lesser extent by pelagic organisms. Since this substance has a relatively long half-life time in sea water, it can be traced throughout the entire water mass. But during the cruise the mean surface water concentration was less than 1 ng/l, which is rather low in comparison to 4 ng/l measured in the Arctic Ocean 1991. And at depths below the productive zone the concentration were frequently below the detection limit (100 pg/l).

In contrast iodinated substances were found more frequently this year than in 1991. An example of the distribution pattern of iodinated compounds is shown in Fig. 6.

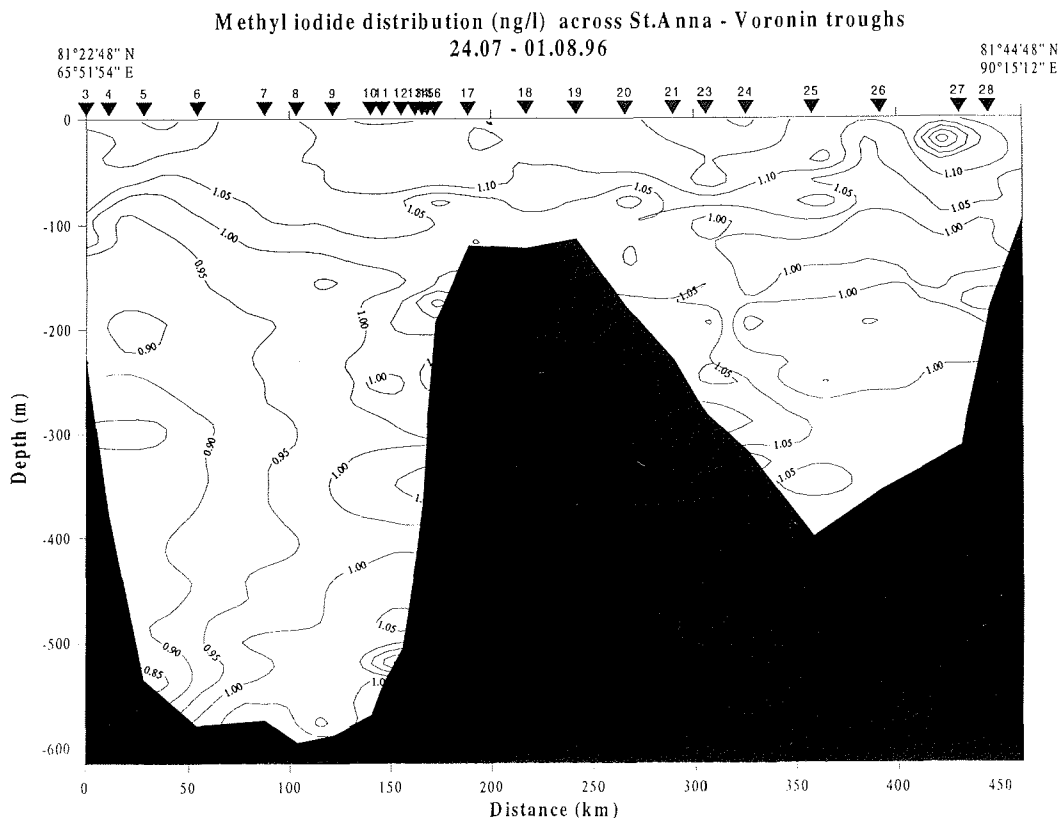


Figure 6: The distribution of Methyl iodide across the St. Anna and Voronin Troughs

### 3.1.9 Dissolved Organic Matter (DOM)

The DOM in marine ecosystems helps to determine the global carbon and nitrogen cycles. DOM in the world oceans has the same order of magnitude as carbon dioxide in the global atmosphere. Of major importance are processes which produce substances which are retained from the carbon-cycle. Humification, e.g. leads to substances which are mostly resistant to microbial attacks. A considerable amount of DOM is transported into the Arctic Ocean through the *Siberian* rivers Lena, Yenisey and Ob. From our samples we intend to investigate the modification of the molecular structures of DOM during its way through the Arctic Ocean.

Water samples were filtered through precombusted glass fibre filters (*Whatman* GF/F), filled into precombusted ampoules and stored in a frozen state. Upon return to *Bremerhaven* the samples will be analysed for:

- dissolved organic carbon (DOC) which will be determined by HTOCO (high temperature catalytic oxidation).
- Humic Substances (HS). Here preparatory work had to be done already on board. Before extraction of the humic substances, seawater samples were filtered through precombusted glass fibre filters (*Whatman* GF/C). 20 l were acidified to pH2 with hydrochlorid acid (*Merck* suprapur). 20 l of the acidified filtrates were passed through the XAD-columns within 24 h. Thereafter, the columns were rinsed with 200 ml of 0.01 N HCl to remove salt. The resins were stored at -30°C. The organic matter of several resins was eluted for further experiments on the bioavailability.

The fraction eluted with base is a so called hydrophobic acid (HbA), and the fraction eluted thereafter with methanol is considered as hydrophobic neutral (HbN).

- Amino acids in the water samples and in the XAD-fractions with the aid of HPLC after precolumn derivatisation with o-phthalaldehyde (OPA) and N-Isobutyryl-L-cystein (IBLC). This method permits the separation of all important D- and L-amino acids. Free amino acids (FAA) will be measured directly, combined amino acids will be hydrolysed with 6 N hydrochloric acid.

3-D-fluorescence spectra of the DOM were recorded for further characterization. Filtered water samples were measured in 1 cm cuvettes with a *Perkin Elmer* LS 50 fluorometer. The excitation range was 200 - 350 nm, the emission range was 230 - 450 nm.

Experiments on the bioavailability of HS were conducted already on board. Natural bacterial population of the corresponding water sample were extracted gently by gravity filtration (0,2  $\mu$ ). The bacteria were then added to artificial seawater supplemented with HS as the only carbon source. To assess the limiting parameters experiments were conducted with different nutrient and HS concentrations. Incubations were done near in situ temperatures (0- -1°C). During two weeks subsamples were taken in certain time intervalls for later analysis of DOC, bacterial numbers and bacterial growth rate

### **3.1.10 Physical and Chemical Speciation of Plutonium (and Americium) in the Arctic Water Column**

The main objective of the Plutonium and Americium analyses is to examine the kinetics of transuranium nuclides reactivity within the Arctic water column and how they are influenced by the chemical speciation and association with suspended particulate and colloidal matter. The overall goal is to achieve an understanding of the basic processes governing the horizontal and vertical dispersion of Plutonium and Americium under extreme environmental conditions.

Particular emphasis was put on the determination of high resolution vertical profiles of Plutonium and Americium in the shelf seas and the central Arctic Ocean, the partition of these radionuclides between filtered and suspended particulate phases, the fraction in colloidal form and the size and composition of the latter. The aim was to obtain a reliable database on radionuclide concentrations in the various water masses, as well as experimental values for the parameters controlling the transfer rate between the water column and the sediment compartments. The values will ultimately be used to refine and validate an existing compartment model covering the Arctic seas and to predict individual and collective doses from potential discharges of radioactivity to these seas. The latter is the goal of a multinational collaboration (ARMARA) involving thirteen *European* institutions.

A total of 75 sea water samples were collected from different depths at 41 stations along the ship's transects. Near-surface sea water samples were taken from approx. 10 m below the surface using the membrane pump located at the ship's bow, while deep waters were retrieved using 10 l *Niskin* bottles mounted in a rosette sampler. In all cases, samples were promptly filtered in situ through membrane (screen) filters (0.45  $\mu$ m) and the filters were retained for analysis of radionuclide content in the suspended particulate fraction. The filtered fractions were then pre-concentrated onboard either for subsequent total Plutonium (and Americium) analysis by co-precipitation with ferric hydroxide according to the method of *Wong et al.* or for Plutonium oxidation state distribution analysis using a scaled-up version of the rare-earth fluoride co-precipitation technique of *Lovett and Nelson*.

Along the hydrographic section between Franz-Josef-Land and Severnaya Zemlya, a total of 32 samples were collected at 14 stations. Sampling concentrated along the eastern flanks of the St. Anna and Voronin Troughs, where water mass outflow from the shelves was anticipated. The analyses included the determination of total Plutonium concentrations, the examination of the oxidation state distribution of Plutonium in filtered sea water at two vertical profiles in the St. Anna Trough and the size fractionation of particle-bound Plutonium in surface waters, including the colloidal component.

The oxidation state distribution of Plutonium in filtered water was examined at two high-resolution vertical profiles taken during the second hydrographic section between the Nansen and Makarov Basins. The samples were collected from two stations located at the deepest parts of the Nansen and Amundsen Basins. Each profile consisted of samples retrieved from eight depths ranging from 10 to 4500 m. On the sections across the Lomonosov Ridge and across the continental slope in the Laptev Sea region, a total of 28 surface and sub-surface samples were taken for total Plutonium and Americium concentrations. Two large volume samples were also collected in order to examine the size fractionation of the colloidal component of these radionuclides by tangential-flow ultrafiltration.

A considerable part of the analysis was conducted already on board of the ship and the final analysis of the samples will be carried out at the *Department of Experimental Physics, University College Dublin*. It is estimated that this will involve a total about 250 separate radiochemical determinations, including reagent blanks and international intercomparisons. Plutonium concentrations in the speciation samples will be determined by high-resolution mass spectrometry, while total Plutonium and Americium samples will be determined using a combination of high-resolution alpha spectrometry and high-resolution mass spectrometry.

### **3.1.11 Acoustic Doppler Current Profiler (ADCP)**

CTD measurements combined with an ADCP were carried out to detect details of water motions associated with small scale temperatures and salinity structures. ADCP/CTD observations were made on the zonal section across the Kara Sea across the continental slope in the Kara Sea sector and across the Lomonosov Ridge between the Amundsen and Makarov Basins.

Two ADCP, one measuring at 150 KHz and the other a 600 kHz, were applied. The first has a range of 250 m, the second a range of 60 m. In the interior of the water column, only relative motions (shears) associated with the interleaving structures can be detected. However, at almost all stations the instruments were run also on a bottom track mode to record motions at the shelf break and at the slopes of the Lomonosov Ridge. During the cruise 54 casts with the *SeaBird* CTD and a RD-ADCP were accomplished. The winch speed was about 40 cm/s in order to get detailed measurements of the fine structure and to achieve a low noise level for the ADCP.

### **3.1.12 Shipborne ADCP**

Vertical profiles of the ocean currents in the topmost 250-350 m of the water column were obtained at most of the hydrographic stations.

The measurements consist of time series which are made up by vertical profiles of one-minute vector-average current values. Typically 2-4 hours long, records were obtained. One observational period exceeded 15 hours in time. Some results from the 15-hour record are presented in Fig. 7. These measurements will supplement

other recent observations of the vertical shear in the upper few hundred meters of the Arctic Ocean. Similar data were obtained from POLARSTERN in the Eurasian Basin in 1993 and 1995, and data have been acquired in the Canadian Basin during summer 1996 by a US Navy submarine. Vertical shear can be used in conjunction with CTD measurements to estimate vertical mixing parameters and to derive vertical fluxes of heat and salt in the upper ocean.

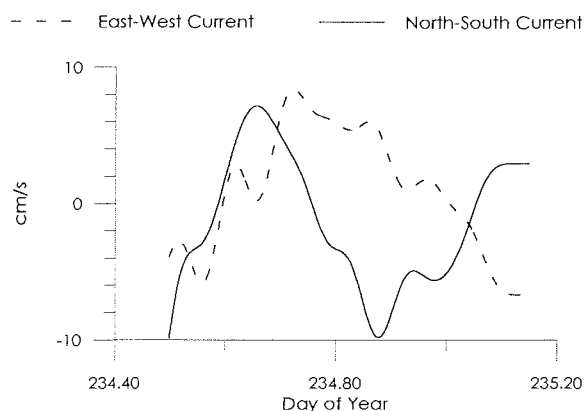


Figure 7: An example of shipborne *Doppler* current measurements below the mixed layer

### 3.1.13 Optics

The optical characteristics of the sea water affect the production of phytoplankton and the absorption of solar radiation in the upper layers of the water column. Ocean colour is furthermore utilized for optical remote sensing in order to determine the surface chlorophyll. Therefore, measurements have been conducted

- to describe optical properties in the Arctic Ocean surface water and
- to explain the observed distributions of chlorophyll, oxygen and phosphate in Arctic surface waters.

Optical measurements in the upper 60 m of the water column were performed at 44 CTD stations where chlorophyll was also analysed.

The following devices were applied:

- Quanta meters for underwater irradiance measurements in the visible wavelength interval of 350-700 nm. One plane quanta meter for relative irradiance. One LiCor spherical quanta meter for the scalar irradiance of the total flux of photons to a sphere (PAR-Photosynthetic Available Radiation). Both were lowered on the same frame equipped with a pressure sensor.
- *Secchi* disc of 50 cm diameter for *Secchi* depth readings of the total backscattered light.

- Colour Index meter to measure the radiance of the backscattered light close to the surface for three different wavelengths (450, 510, 550 nm).
- Quantum sensor to measure Photosynthetic Photon Flux Density (PPFD) in the atmosphere as reference during the underwater measurements.

The estimate of the *Secchi* depth by eye was made at about 6 m above the sea surface. Quanta measurements were mostly made during overcast conditions. The quanta meter readings will be analysed together with the readings of the deck quanta. The incoming daylight during station time varied between 942 and 51  $\mu\text{mol m}^{-2}\text{s}^{-1}$ .

As a result of absorption and scattering of the solar flux the irradiance diminishes in an approximately exponential manner. The exponential decrease of quanta at two stations is shown in Fig. 8. Station 29 has more chlorophyll in the upper oceanic layer than station 80, *Secchi* depths readings in Arctic waters are highly dependent on the particle content of the water and less on dissolved (yellow) substances. The particles could be of both organic and inorganic origin. The *Secchi* depth ( $Z_s$ ) gives a rather good approximation of the light attenuation.

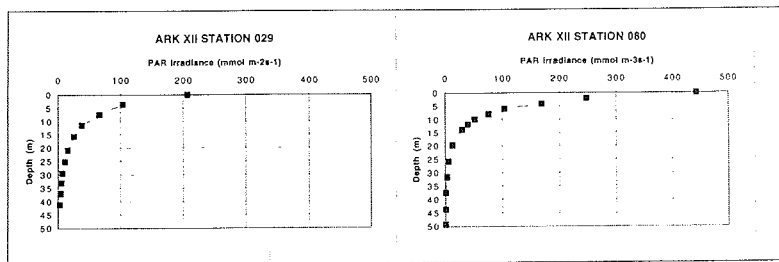


Figure 8: Vertical profiles of the photosynthetic available radiation (PAR)

The Colour Index meter is designed to measure the underwater light regime independent of clouds, sun elevation, waves and ship shading. It contains two photocells equipped with interference filters of 450 nm, 520 nm and 550 nm that face downward to record nadir radiances. The Colour Index, defined as the radiance of blue (450 nm)/radiance of green (520 nm) yields information about the quanta distribution in the whole euphotic zone. Thus, from the colour index it is possible to calculate how deep light penetrates. The averaged colour index for all 44 stations is 2.14 at 1.5 m depth. The depth of the euphotic zone calculated from the colour index for all 44 stations is 60 m.

### 3.1.14 Ocean Moorings

Three highly instrumented moorings had been deployed one year ago at the continental slope of the Amundsen and Makarov Basins and at the *Eurasian* side of the Lomonosov Ridge (Fig. 2) at depths around 1700 m.

Each mooring was equipped with current meters at 100, 270, 700, 1100 meters depth and at 20 meters above the bottom. At the two uppermost and at the deepest levels *Sea Bird* SBE-16 (SeaCats) instruments were also installed to measure the

conductivity and temperature. The depths were chosen to monitor the halocline (100 m), the warm Atlantic core water (270 m), the Barents Sea inflow (700 m and 1100 m) and to detect currents of dense bottom water originating from the shelves. Two of the moorings carried upward looking sonars to determine the draft of sea ice. The mooring at the Lomonosov Ridge was furthermore equipped with two sediment traps at 150 m depths and at 150 m above the bottom.

The current meters and the SeaCats of all moorings and one upward looking sonar have operated continuously. Each sediment trap has collected twelve monthly samples. The recovered instruments will be calibrated and the data will be reduced by the owners of the various instruments. Preliminary current meter data (converted onboard) are portrayed in Fig.9.

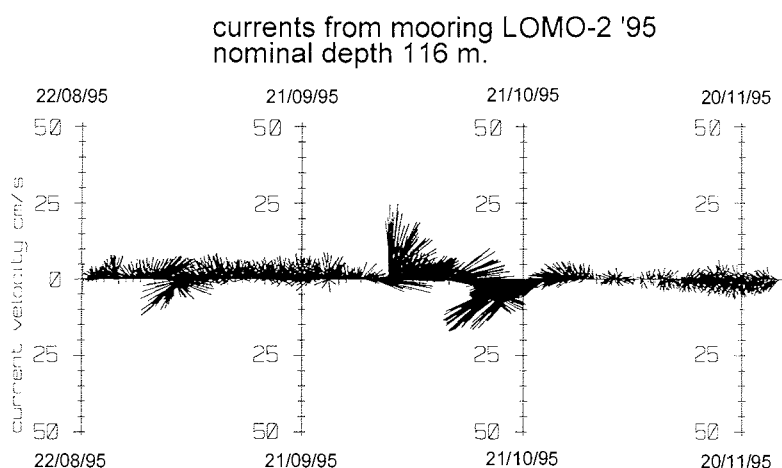


Figure 9: 3 days time series of current vectors at the mooring LOMO-2

### 3.2 Oceanographic / Meteorological Buoys (AWI, AARI)

Eight drifting surface buoys were deployed at positions indicated in Fig. 10. The positions of the drifting buoys are determined by the Global Positioning System (GPS). All buoys, except one, are equipped with sensors for air temperature and air pressure. Two buoys are additionally equipped with ice thickness sensors, two others with anemometers at 2 m height. Five buoys have been deployed in an array of 160 km diameter. The central two buoys carry a 200 m long subsurface chain with sensors for water temperature, conductivity, pressure and current velocity. These two buoys were deployed 8 km apart on one large ice floe in order to record small scale coherent oceanic features. All data are transferred in real time to the Global Telecommunication System (GTS) and are thus available for weather forecast purposes.

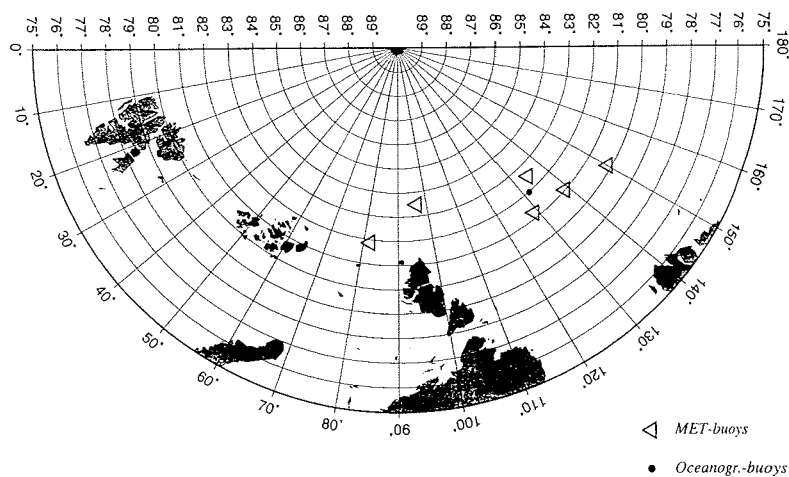


Figure 10: Positions of automatic meteorological surface buoys (triangles) and two oceanographic systems (dot)

### 3.3 The Atmospheric Boundary Layer (AWI, IMKH, AERODATA, AARI, OAP)

Fluctuations of the wind velocity, the air temperature and moisture were measured to document the structure of turbulence in the polar atmosphere and to improve the parameterization of the subgridscale processes in atmospheric models of different spatial resolution. Measurements were carried out with the aid of a new sophisticated instrument, the HELIPOD, which is mounted on a 15 m long cable below the cabin of a helicopter and with a turbulence measuring system (TMS) which is installed at a vertical mast at the ship's bow crane. The TMS records turbulent fluxes of heat and momentum in 5 different levels between 3 m and 20 m height above the sea surface with sonic anemometers / thermometers. And humidity fluctuations are detected by a *Lyman* alpha sensor at 3 m height. In addition the absolute humidity is measured by a dew point mirror and the vertical profiles of air temperature are obtained from PT-100 temperature sensors also at 5 levels.

The HELIPOD is able to measure wind vector, air temperature and moisture fluctuations with a time resolution of 100 Hz. Since the motions of the sonde are recorded simultaneously by special devices accurate values of the turbulent quantities can be determined. The system is designed, to work autonomously. To correct for any time drift of the fast sensors highly stable slow sensors are measuring temperature and relative humidity in parallel.

During Arctic '96 the TMS could be operated at 35 ship stations on 24 days. The minimum observational time lasted about 2.5 hours in order to achieve a satisfactory statistical accuracy. 24 HELIPOD flights were carried out on 20 days. Flight patterns to determine vertical flux profiles and surface fluxes are portrayed in Fig. 11. Surface fluxes have been mainly determined from flights in about 10 m height, for horizontal averages of more or less 30 km. The ice topography was measured simultaneously by a laser altimeter. Vertical profiles of the fluxes have

been gained from box patterns with side lengths of 8 km. The flight levels ranged from 7.5 m height to the top of the atmospheric boundary layer (approx. 100-200 m).

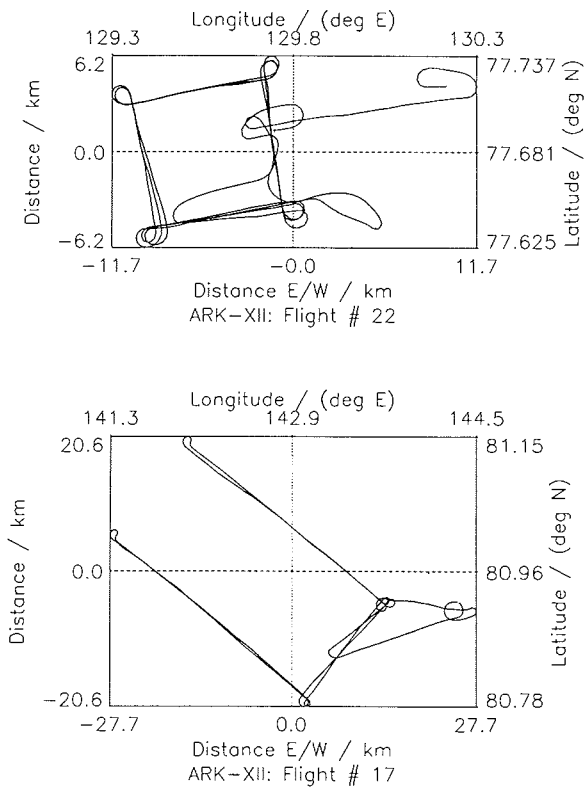


Figure 11: Actual helicopter flight pattern. Repeat tracks refer to different flight levels

Turbulence measurements could be made on a large part of POLARSTERN's route (Fig. 12) so that the data are representative for summertime atmospheric conditions over the *European Arctic Ocean*.

Most of the observations were carried out when ice concentrations ranged above 80 %. Nevertheless inhomogeneous surface temperatures prevailed due to changes of ice thickness and to the effects of leads. Furthermore, the low level air flow was affected by the surface roughness caused by ice ridges and the edges of ice floes. Consequently, the surface layer was frequently well mixed while the upper part of the atmospheric boundary layer starting at 20 to 30 m height was stably stratified. In a few cases slightly stable or unstable density distributions were met also near the lower boundary of the atmosphere.

TMS and HELIPOD measurements, ARK XII from 25.07.96 to 05.09.96

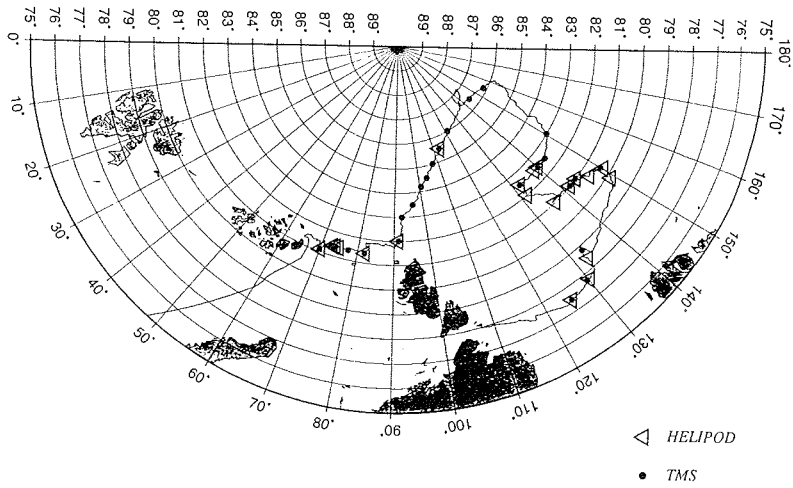


Figure 12: Positions where turbulence measurements were carried out with the HELIPOD (triangles) and with the profile mast at the ship's bow crane (dots)

Typical profiles of the turbulent fluxes are shown for two days (July 30 and August 20), when simultaneous measurements were carried out with the TMS and the HELIPOD (Fig. 13).

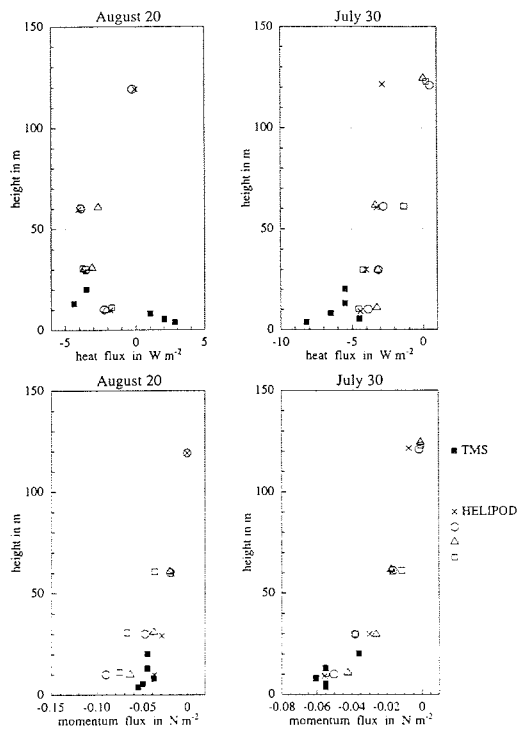


Figure 13: Vertical distributions of turbulent heat and momentum fluxes

The TMS values represent time averaged data over a period of about 45 minutes, the HELIPOD-data are horizontally averaged over some 30 km. The momentum fluxes of the two different systems fit rather well while the sensible heat fluxes seem to indicate some disagreement. But detailed inspections of the boundary conditions at the ship convinced us that local surface temperatures which differ distinctly from area averages have caused the observed differences. In particular on 20 August the ship's bow was located over a small lead which obviously created a local low level internal boundary layer. In several other cases out of a total of ten the results of both systems agreed closely.

Six experiments have been carried out to study internal boundary layers, which evolve during the passage of the airflow from the ice edge towards open water. For these purposes POLARSTERN was moved at a low speed of about 0.5 knots upwind across the lead towards the ice edge.

During the study on 8 August the water surface temperature was lower than the ice surface temperature so that a thin stable layer was present downstream over the water as illustrated in Fig. 14, which displays the momentum and sensible heat fluxes, the local drag coefficients (defined as the square of local friction velocity divided by the local windspeed) and the local stability function  $1/L$  ( $L$  is the Monin Obukhov stability length), as observed with the TMS.

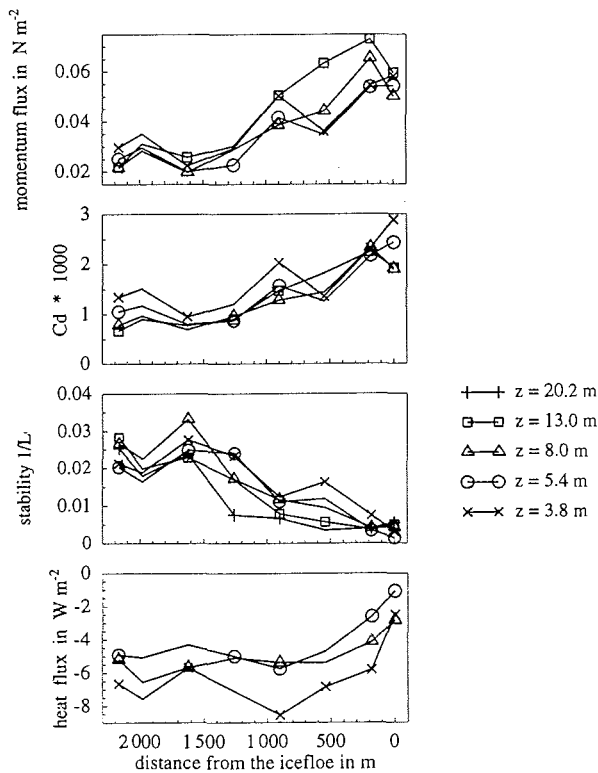


Figure 14: Turbulent momentum (upper panel) and heat (lower panel) fluxes as well as the drag coefficients ( $Cd$ ) and the static stability function ( $1/L$ ). For details see text

### 3.4 Sea Ice Physics and Biology (AWI, IPÖ, AARI, GU, HUT, SPRI)

#### 3.4.1 Visual Ice Observations

Visual ice observations were made from the ship's bridge every two hours when steaming through the ice. Concentrations of different ice types, ice thickness, snow thickness, flow size, lead width, melt pond distribution and ridging characteristics were observed. In addition, concentration of the sediment laden ice and the amount of ice algae were estimated. The total ice concentration versus time is displayed on Fig. 15.

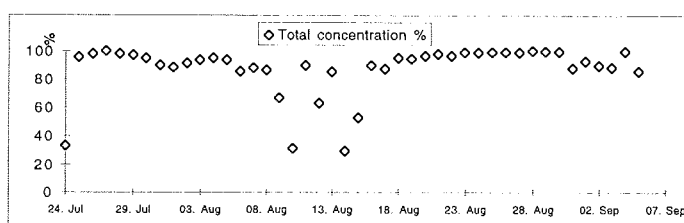


Figure 15: Total ice concentration

After 15 August the formation of new thin ice (Fig. 16) began already.

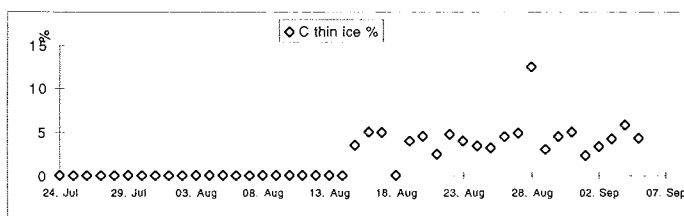


Figure 16: Concentration of thin ice

The main feature on Figure 15 is the low concentration between 9 and 15 August during the northern most section of the cruise which is also obvious on the AVHRR image in Fig. 17. In this area second-year or multiyear ice was predominant (Fig. 18) and the snow cover amounted to 40 cm. According to the one year's drift of three ARGOS surface buoys (Fig. 19) the sea ice we met in the most northern area was formed in the Laptev Sea area at least one year ago. Summer surface melting conditions were observed only in the northern Kara Sea and in the southern Nansen Basin.



Figure 17: AVHRR image of the expedition area; cruise track: white line

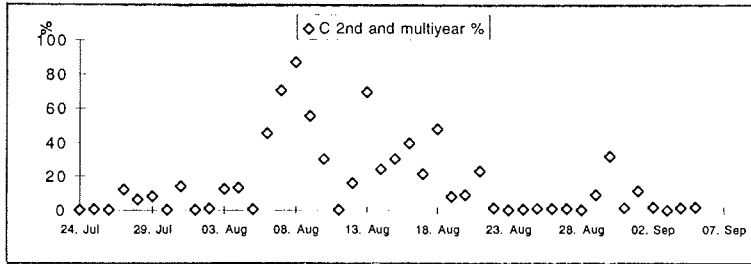


Figure 18: Concentration of second and multiyear ice

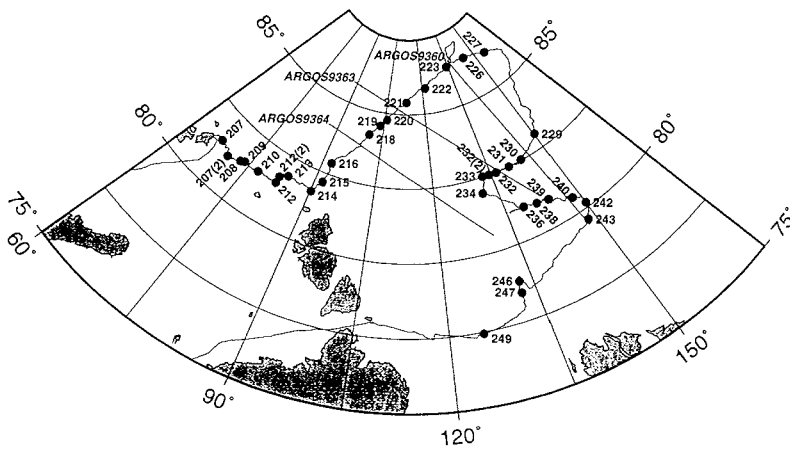


Figure 19: Cruise track with indications of Julian days, three straight lines are connecting the starting and actual positions of ARGOS-tracked buoys

### 3.4.2 On Ice Measurements

Measurements on the ice were performed on 37 floes. The geographical locations of these stations are indicated in Fig. 19. Ice station work comprised ice thickness measurements, ridge sail levelling and partly ice core drilling. The cruise track provided a unique opportunity to study different states of the ice cover upstream of the Transpolar Drift.

### 3.4.3 Laser Altimetry

The ice surface topography was frequently determined with a vertically downward looking laser altimeter mounted on a helicopter. The instrument was flown with a speed of 80 kn at a height of 30 m above the surface. The pixel spacing was about 0.02 m. Typical flight patterns were equilateral with a side length of 20 nautical miles. 23 flights were performed with a total profile length of about 2000 km. Additionally, some laser altimeter data were obtained during the HELIPOD flights. The data quality is expected to be high due to the absence of melt ponds and to the closed snow cover.

The measurements will be primarily analysed for pressure ridge statistics. The data will also serve as ground truth values for satellite radar altimeter measurements as well as for comparisons with the ice draft values derived from the upward looking sonars (ULS) of the ocean moorings. A ridge height distribution for a flight across one mooring site is demonstrated on Fig. 20. The height distribution will be compared to the keel depth time series measured by the moored ULS.

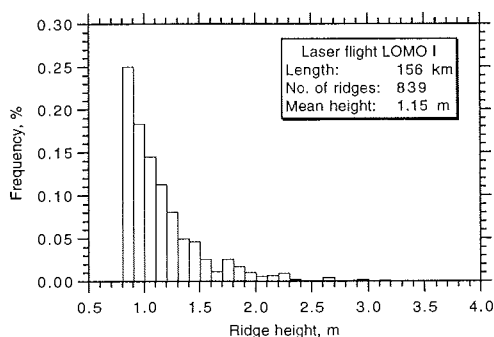


Figure 20: Ridge height distribution obtained from a laser altimeter flight

### 3.4.4 Ice and Snow Thickness

At 35 positions ice thickness was measured along linear profiles covering both level and deformed ice by means of an electromagnetic inductive (EM) technique. The EM instrument (coil spacing 3.66 m, signal frequency 9.8 kHz) was mounted into a kajak which was pulled over the ice. On average, the thickness profiles extended over at least 1000 m with a point spacing of 5 m. In addition, snow thickness and surface elevation (by means of levelling) were determined with a similar spacing along the first 200 m of the profiles and ice thickness was measured

along these short sections by drilling at 20 m distance intervals to calibrate the EM soundings. The mean and modal total thickness for all stations as well as the standard deviation together with minimum and maximum values are shown in Fig. 21. These thicknesses compare rather well with the mean ice thickness determined from video images taken at the ship's bridge. From our observations six different ice regimes can be distinguished which are indicated in Table 1 and displayed in Fig. 22.

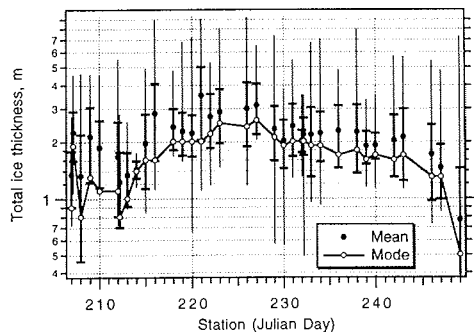


Figure 21: The thickness distribution along the cruise track

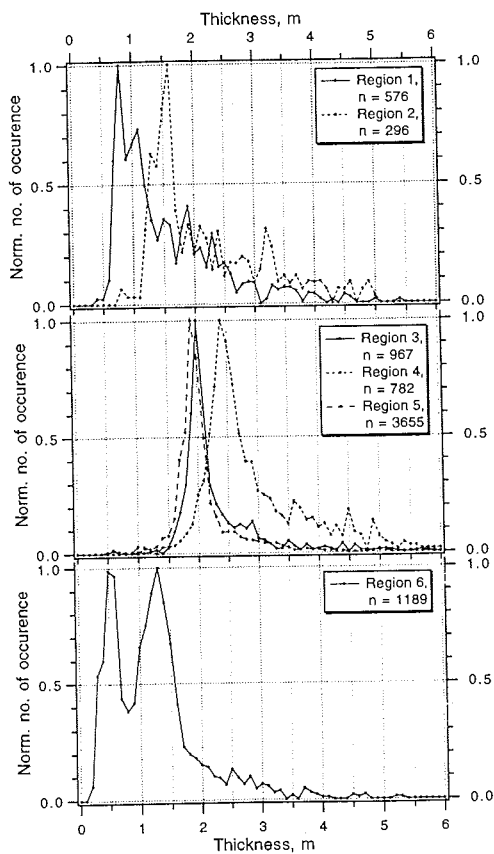


Figure 22: Standardized ice thickness spectra for 6 different regions of the Arctic Ocean

All sampled floes were covered by old snow and in the northerly regions also by fresh snow on top. The snow was thickest around ridges, thus smoothing their relief. Measured mean snow thicknesses and their standard deviations are also listed in Table 1. The mean density of 31 samples of old snow was  $407 \pm 73 \text{ kg/m}^3$ .

**Table 1:** Subdivision of the cruise track into six regions showing different ice and snow thickness characteristics (see also Figure 21)

Region	Stations	Mean Total Thickness	Mode	Mean Snow Thickness	Std. dev.
1 Kara Sea	207-213	$1.64 \pm 49\%$	0,8	0.08	0.10
2 Nansen Basin	214-216	$2.37 \pm 48\%$	1,6	0.07	0.09
3 Transpolar Drift, west	216-221	$2.50 \pm 38\%$	2	0.21	0.16
4 Transpolar Drift, east	222-227	$3.02 \pm 33\%$	2,4	0.26	0.15
5 Transpolar Drift, south	229-243	$2.13 \pm 31\%$	1,9	0.14	0.12
6 Laptev Sea	246-249	$1.29 \pm 58\%$	1,3	0.10	0.06

### 3.4.5 Ridge Sail Profiles

The topography of the maximum height along pressure ridges was measured on most ice stations by a laser levelling device at 1 m intervals (Fig. 23). Generally data on ridges are obtained from transects across the ridges by aircraft laser altimetry and keel depths are measured by submarine sonars so that the sail heights or keel depths are random samples of the actual values. With the aid of the sail profile statistics these data may be converted into more realistic ridge thickness values.

A total number of 25 ridges with a total length of 3.2 km was investigated. The maximum elevation found was 5.6 m and the mean elevation amounted to 3.1 m. Cross-sectional profiles were measured on 7 stations with special emphasis on the detection of the snow thickness (Fig. 24).

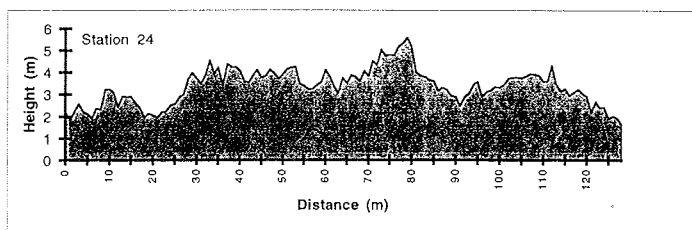


Figure 23: Topography of a pressure ridge along its axis

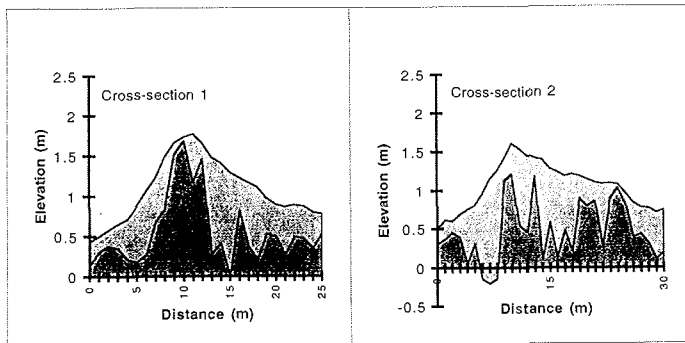


Figure 24: Topography of snow covered pressure ridges across their axes

### 3.4.6 Trafficability

When POLARSTERN was steaming in the pack-ice ship performance data were analysed together with ice thickness, lead width, floe size and ridging information. A considerable portion of the icegoing time was needed for ramming as can be concluded from Fig. 25. However, significant correlations were observed neither between the ridging intensity and the number of rammings per nautical mile nor between the ship performance and ice thickness. This is due to the fact that the ship proceeded along leads, whenever possible. But the number of rammings clearly depends on the lead width (Fig. 26). When the latter was small and many floes were compressed the ship had to ram frequently and even got repeatedly stuck. From 21 to 31 August the ship got stuck 15 times.

In addition to the ship's performance one hour observations were made for five different ice conditions for ice resistance calculations. During these occasions the local ice conditions and all ship-ice contact events were recorded, the thickness was monitored continuously and the thrust, propeller pitch and torque were logged in one minute intervals.

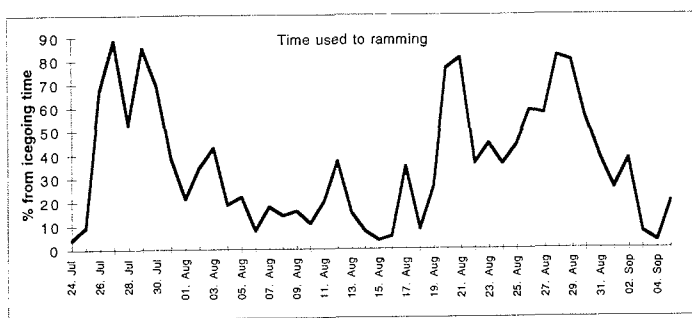


Figure 25: Percentage of daily time required for ramming

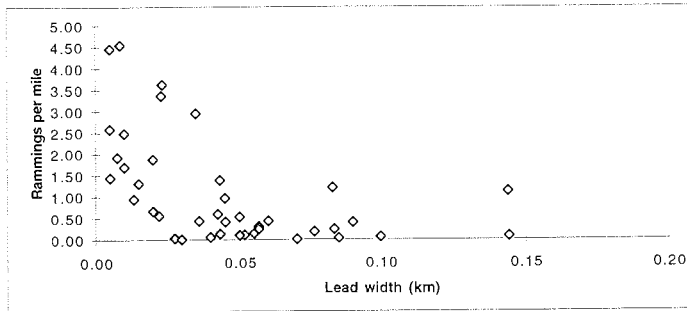


Figure 26: Number of rammings per mile of progress versus lead width

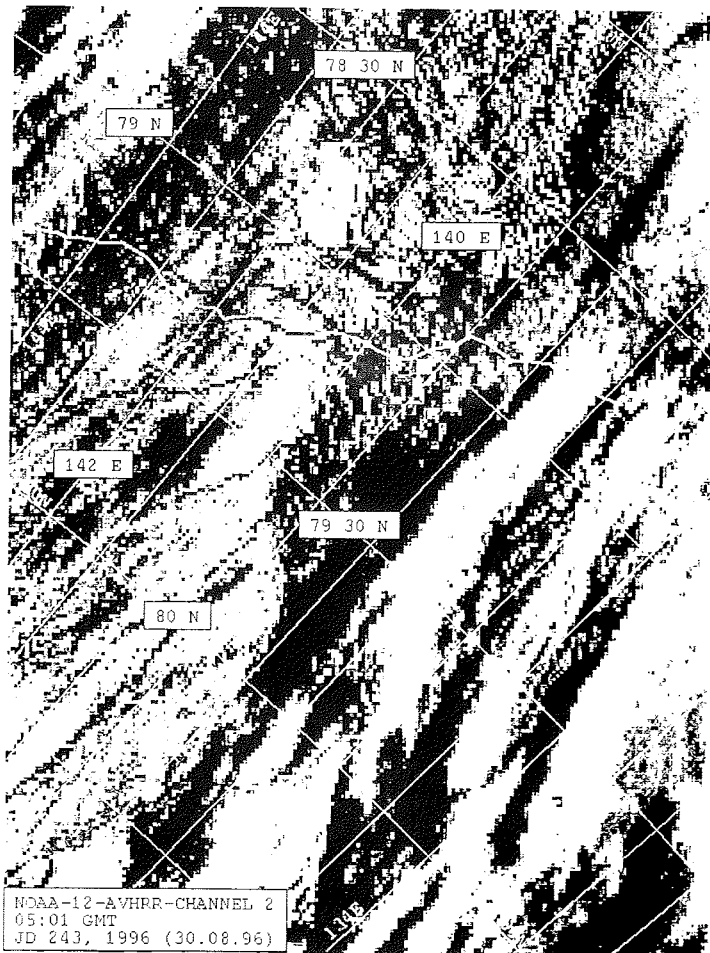


Figure 27: Magnified AVHRR image distinctly showing long leads in the sea ice

### 3.4.7 Sea Ice Remote Sensing

A HRPT (High Resolution Picture Transmission) system on board POLARSTERN received AVHRR data of the NOAA-Satellites 12 and 14 from approximately 300 overpasses. The images were used to monitor the ice conditions along the cruise track and to support the ship's navigation. Later the scenes will be evaluated together with satellite data from the ERS-SAR and from the radar altimeter. An example of the obtained images is portrayed on Figure 17. The enlargement of the southern Laptev Sea on Fig. 27 reveals wide and rather long leads within the otherwise closed ice cover. This information was used to optimize the ship's route in these basically severe ice conditions. Comparing the track of POLARSTERN with the satellite image taken some hours earlier some hints on the ice drift can be obtained. In addition to the NOAA data 21 images from the OKEAN satellite were received and stored for later analysis.

To improve the algorithms for satellite passive microwave signals of sea ice, radiometric measurements were performed near the ice surface.

The passive microwave signal of first-year and second-year ice was measured at 15 stations at frequencies of 11, 21, 35 and 37 GHz with horizontal and vertical polarization under different environmental conditions (Table 2). 3 microwave-radiometers (11, 21, 35 GHz) of the *University of Bern (Switzerland)* and one of the *Arctic and Antarctic Research Institute, St. Petersburg (Russia)* were applied.

**Table 2:** Radiometer Stations

Station No.	Date	Radiometric Measurements
41/018	28.07.	11,21,35 GHz 20-70 deg., FY-ice,frozen puddle
41/022	30.07.	11,21,35 GHz 20-70 deg.
41/029	01.08.	11,21,35 GHz 20-70 deg.
41/043	05.08.	11,21,35 GHz 20-70 deg.
41/046	06.08.	11,21,35 GHz 20-70 deg., 50 deg. profile 12 m
41/048	07.08.	11,21,35 GHz 20-70 deg., profile 3 m
41/052	08.08.	11,21,35 GHz 20-70 deg., 50 deg.with and without fresh snow layer
41/055	09.08.	11,21,35 GHz 20-70 deg.
41/073	16.08.	11,21,35 GHz 20-70 deg., 50 deg.with and without metal sheet
41/080	19.08.	11,21,35,37 GHz 20-70 deg.
41/083	21.08.	11,21,35,37 GHz 20-70 deg., 50 deg. profile 10 m (11,21,35 GHz, snow thickness)
41/088	25.08.	11,21,35 GHz 20-70 deg., 40,50,60,70 deg. profiles 15 m, snow thickness
41/090	26.08.	11,21,35 GHz 20-70 deg., 20,45,55,60 deg. profiles 5 m, 50 deg. profile 15 m, snow thickness (new snow, refrozen snow)
41/100	02.09.	11,21,35 GHz 20-70 deg., 50 deg. profile 55 m, snow thickness
41/103	03.09.	11,21,35 GHz 20-70 deg., 50 deg. profile 40 m, 30,40,60,70 deg. profiles 3 m

The radiometers were installed on a sledge at a height of about 1.8 m over the ice surface. The angle of incidence could be changed between 20 and 70 degrees in steps of 5 degrees.

Additionally, profile measurements with a typical point spacing of 0.5 m were performed to analyse lateral changes in the microwave emissivity. The microwave signals along these profiles correlated significantly with the snow thickness. Detailed values for two floes are reproduced in Tables 3 and 4

The signals of the different channels are obviously closely correlated.

**Table 3:** Correlation coefficients for measurements at station 41/103

	11h	21h	35h	11v	21v	35v	SnowTh		
11h	1.000		0.939		0.899		0.972	0.954	0.904
	0.665								
21h	0.940	1.000			0.981		0.921	0.989	0.975
	0.757								
35h	0.899	0.981	1.000		0.879		0.879	0.970	0.995
	0.786								
11v	0.972	0.921		1.000			1.000	0.951	0.890
	0.690								
21v	0.954	0.989		0.970	1.000		0.951	1.000	0.975
	0.755								
35v	0.904	0.975		0.995	0.890	1.000	0.890	0.975	1.000
	0.783								
SnT	0.665	0.757		0.786	0.690	0.755	0.690	0.755	0.783
	1.000								

**Table 4:** Correlation coefficients for measurements at station 41/100

	11h	21h	35h	11v	21v	35v	SnowTh		
11h	1.000		0.680		0.630		0.890	0.686	0.633
	0.367								
21h	0.680	1.000			0.955		0.804	0.967	0.940
	0.523								
35h	0.630	0.955	1.000		0.730		0.730	0.933	0.977
	0.446								
11v	0.890	0.804		1.000			1.000	0.842	0.771
	0.515								
21v	0.686	0.967		0.933	1.000		0.842	1.000	0.960
	0.427								
35v	0.633	0.940		0.977	0.771	1.000	0.771	0.960	1.000
	0.410								
SnT	0.367	0.523		0.446	0.515	0.427	0.515	0.427	0.410
	1.000								

### 3.4.8 Biological and Physical Sea Ice Properties

A total of 185 ice cores were taken at 23 locations for physical and biological investigations. Temperature, salinity, chlorophyll and meiofauna-organisms were determined. Grazing and growth rates of sea ice organisms were derived and cultures of sea ice organisms were established for future experiments. Three plankton samples were taken with a 20  $\mu\text{m}$  net from the ice edge for comparisons with the pelagic community in the underlying water column. In addition, one sample was taken from new ice to investigate the colonisation by meiofauna organisms.

Cores were drilled with a KOVACS ice corer (10 cm diameter). Ice temperatures were measured every 10 cm with a digital temperature probe inside the core immediately after drilling. The same core was then cut into 10 cm segments. The melted segments were analysed for salinity and chlorophyll. Additional ice cores from the same site were cut into 10 to 2 cm thick segments for investigations on sea ice biota. For meiofauna-studies, the segments were melted in an excess of 0,2  $\mu\text{m}$  filtered sea water at 4°C to avoid osmotic stress to the organisms. After complete melting, the sample was concentrated over a 20  $\mu\text{m}$  sieve and either sorted alive under a dissecting microscope or fixed with *Bouin's* solution or formalin (1% end-concentration) for later sorting and taxonomic studies. Cultures of sea ice organisms were established from melted samples in culture flasks under a light-dark-cycle of 12:12 hours. Average core salinities between 3 and 4 ‰ (Fig. 28) dominate the sample and the salinity profiles which are characteristic of summer desalinated ice, i.e. the upper 30 - 50 cm comprises very low salinities with slightly higher values below (Fig. 29). Four cores with average salinities < 2‰, were taken from areas of refrozen melt ponds and one core with an average salinity of 5.2 ‰ was taken from a site near the floe edge.

The temperature profiles were determined by the relatively high air temperature near the top and the freezing water temperature at the bottom. The density of core segments was calculated from volumetric and mass measurements. The average density for all segments was 876.3  $\text{kgm}^{-3}$  with a maximum of 988.4  $\text{kgm}^{-3}$  and a minimum of 716.9  $\text{kgm}^{-3}$ . All density profiles showed a trend of increasing density with core depth. From these bulk properties, the brine and gas volumes of the cores can be calculated.

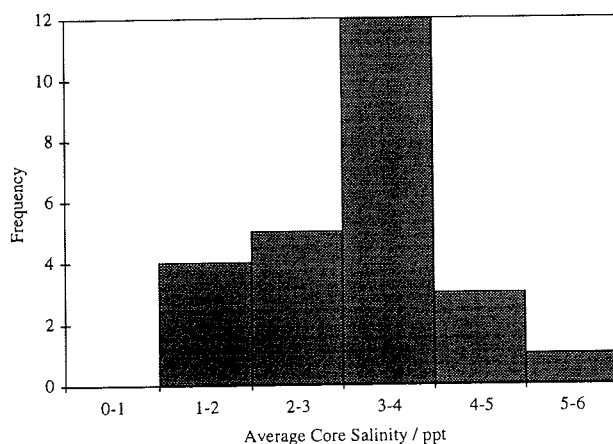


Figure 28: Mean Salinity distribution in sea ice cores

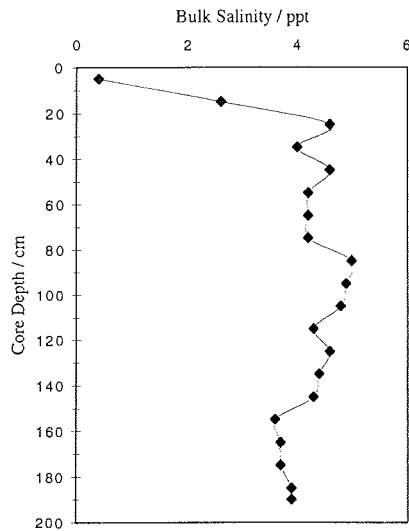


Figure 29: Typical vertical salinity profile in sea ice during ARCTIC '96

At 17 stations, the temperature and salinity of the underlying water columns was measured using a portable conductivity-temperature (CD) device. The probe was passed through the bore hole on a graduated cable and the CD profile of the water was measured to a maximum depth of 15m. It was anticipated that a sharp halocline would be observed where fresh melt water overlies the more saline oceanic surface water. This feature was not observed at any of the stations and all profiles showed a uniform salinity over the full depth. Measured salinities ranged from 34.2‰ to 32.3‰. This absence of under ice melt water may be explained by the low surface ablation. The salinity of surface water along the cruise track (Fig. 30) is separated into two distinct groups; stations 207-220 with an average 33.9‰  $\pm$ 0.3 and stations 223-246 with an average 32.7‰  $\pm$ 0.3. The saline Barents Sea water (207 - 220) differs from the fresher surface layer which is likely to be modified by river run-off. Variability within these two groups is attributed to salinity variations by melt water. The meiofauna community is dominated by ciliates but rotatoria and a few nematodes are also present as indicated in Fig. 31 and 32. Highest concentrations of organisms occur in the lowermost centimetres, but in core 208-07 a relatively high concentration of ciliates was also found in the upper 20 cm. Compared to earlier investigations, the abundance of metazoans in the ice community of these cores was lower, but whether this holds true for the whole region has to be seen from the remaining samples.

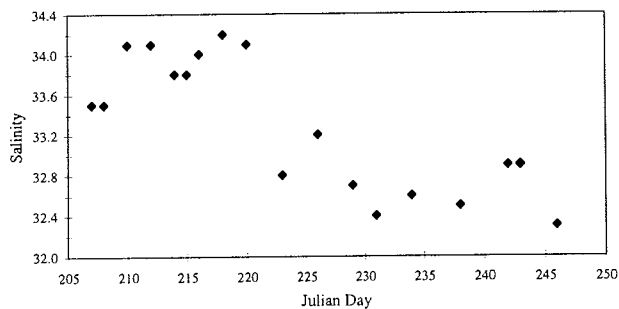


Figure 30: Surface water salinity along the cruise track

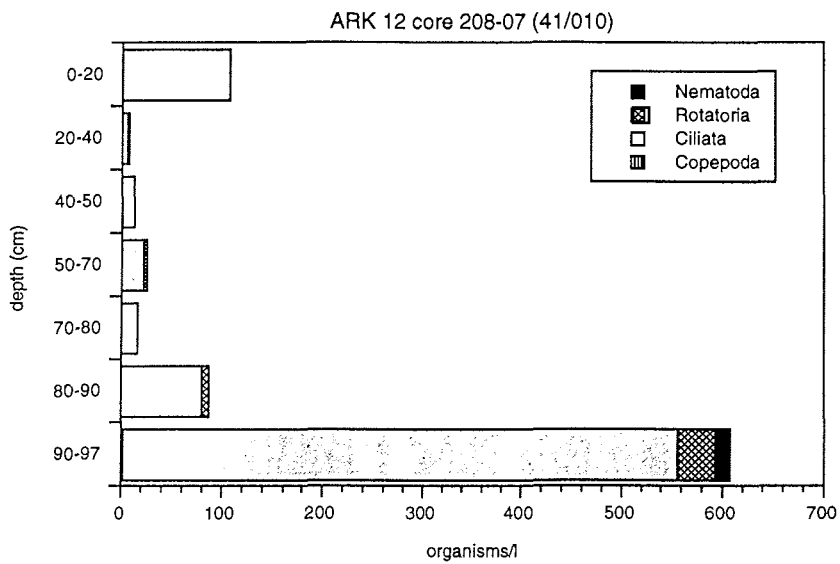


Figure 31: Depths distribution of the detected meiofauna in sea ice

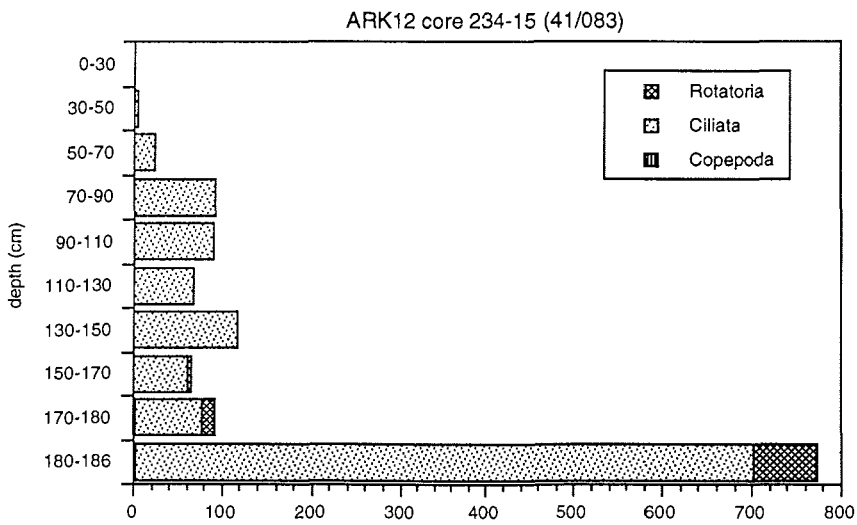
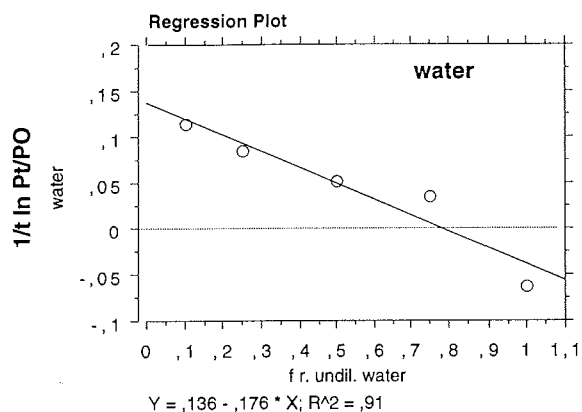


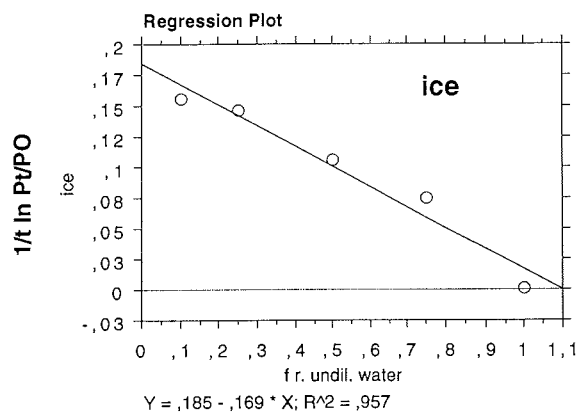
Figure 32: Same as Fig. 31

Sea ice organisms are generally small in size due to the structure of their habitat, the brine pockets and channels inside the ice. Small protozoans and metazoans are regarded to have a disproportionately high rate of growth, metabolism and feeding, so their role in the "in ice food web" may be significant. Quantitative information about fluxes of organic carbon is restricted to measurements of total production of algae and bacteria using radioactive tracers. In most of these experiments ice organisms are kept in water, and the influence of ice is neglected.

Serial dilution experiments (*Laundry and Hassett 1982*) were conducted to estimate growth and feeding rates of ice organisms. For this purpose ice core sections were melted and sea salt was added. In 14 out of a total of 28 serial dilution experiments ice was present in the bottles. The experiments were run over periods of 3 to 10 days in an incubator at about -2°C and with a 20 - 40 mE m-2s-1 light intensity (PAR). Growth and grazing rates were calculated from biomass measurements (chlorophyll a) and cell counting (Fig. 33).



doubling time autotrophe organisms: 7,35 days, grazing rate: 5.68 days



doubling time autotrophe organisms: 5.40 days, grazing rate: 5.91 days

Figure 33: Apparant growth in serial dilution experiments of ice organisms in pure water (top) and in water with ice (bottom)

### 3.5 Marine Biology (AWI, IPÖ, AARI, MMBI)

#### 3.5.1 Phyto- and Zooplankton Ecology and Vertical Particle Flux

The distribution of phyto- and zooplankton in the water column was measured along the entire cruise track to extend the existing data bases of the Arctic shelf seas which were collected during the recent years.

Of particular interest are:

- regional differences in the seasonal distribution patterns of phyto- and protozooplankton as well as interannual variations,
- the influence of the physical and chemical conditions and of nutrient availability on marine primary and secondary production,
- the effects of sea ice on the pelagic food web,
- the relationship between algal biomass and grazing pressure,
- the vertical transport of organic matter into deeper layers and to the sea floor.

At 54 oceanographic stations water samples were taken by the rosette sampling system. On each station subsamples were obtained at twelve discrete depths from the surface (2.5 m) down to the 300 m - layer for the following values:

- Chl-a and phaeopigments: Pigment concentrations were measured on board with a *Turner Design Fluorometer* after filtration of the samples, homogenisation and cold extraction in 90% acetone.
- Species abundance: Samples (ca. 200 ml) were fixed with hexamine-buffered 37,5% formalin (final concentration 1.0%). Microscopical analyses will be carried out in the home laboratory to investigate the distribution of the phytoplankton.

At fewer stations additional samples were obtained in the upper 300 meters and in deeper layers to determine:

- Particulate organic carbon / nitrogen and biogenic silica: Samples were filtered on precombusted glassfibre filters (POC/PON) or cellulose acetate filters (silicea) and stored at -20°C for later analysis in the home laboratory
- Proto- and microzooplankton as well as fecal pellets. The samples were fixed with hexamine-buffered formalin (final concentration 2%) and will be analysed under the microscope at home laboratories.

Furthermore at the position 81° 4.5'N / 138° 54.0'E two moored sediment-traps (150 m below the surface and 150 m above the sea floor) were recovered which had been deployed one year ago to analyse the seasonal vertical flux of matter down to the bottom. Both traps had functioned accurately and the secured samples were stored at 4°C, they will be analysed at home for the seasonal particle-flux.

- Seston samples: The samples were filtered on preweighted glassfibre and stored at -20°C for later analysis in the home laboratory.

#### 3.5.2 Biomass Distribution (chlorophyll-a)

In general the chlorophyll-a values were quite low at positions with a high ice coverage. The level of 1 mg/l was never exceeded except on station 3 (see below), therefore no bloom event could be observed. Almost no chlorophyll-a was found in depths larger than 100 m.

On station 3 near Franz Joseph Land maximum-values for chlorophyll-a were detected (Fig. 34). The higher concentration was reached in the upper 20 m with 1.92 mg/l. Most stations were dominated by higher values in the upper 10 to 20 m and an exponential decrease in the depths below. The profile at station 12 is typical for the chlorophyll-a distribution on the transect across the St. Anna and Voronin Troughs.

In the deep basins the values were generally smaller than 0.2  $\mu\text{g/l}$ . Only the values at station 58 with an ice concentration of only 20% surmounted this limit. The profile of station 62 under 60% ice cover is more typical for the inner Arctic. Continental slope: At the continental slope of the Laptev Sea chlorophyll-a increased again up to 0.4  $\text{mg/l}$  in spite of an ice coverage of about 90%.

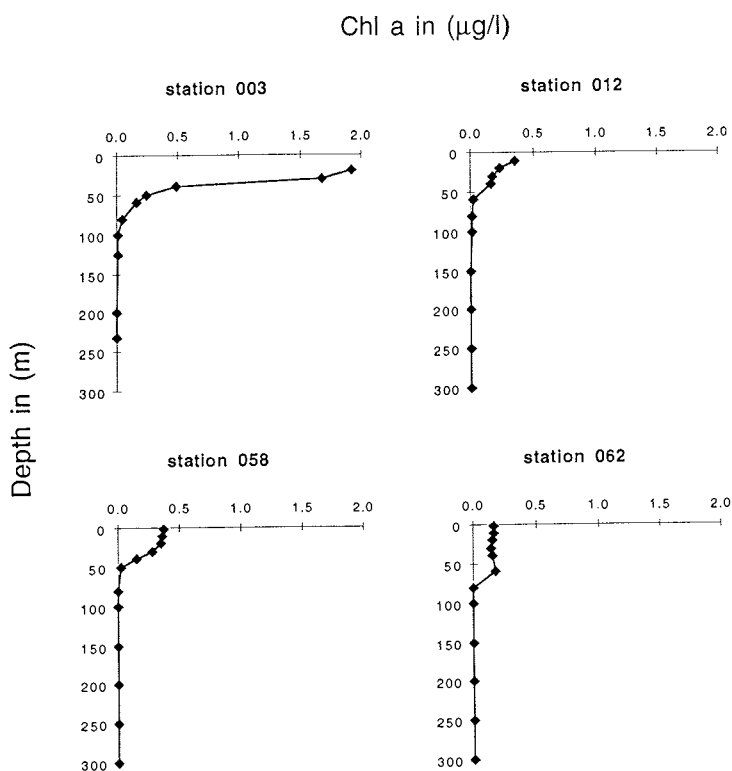


Figure 34: Vertical chlorophyll-a-distribution in 4 different regions

### 3.5.3 Taxonomy and Spatial Distribution of the Microplanktonic Community

The samples of sea water obtained during the entire cruise were analysed for mikroplankton. 200 ml of water were taken from the rosette sampler and preserved with 1% *Lugol* solution. After 3 days of sedimentation the samples were concentrated to the volumes of 2 - 3 ml. Identification and enumeration of mikroplanktonic organisms larger than 15  $\mu\text{m}$  were carried out in the 0.1 ml counting chamber under the *Amplival* microscope. Size parameters of cells of flagellates, ciliates and of most diatoms were measured individually with the ocular micrometer at the magnification of 400 and then biovolumes were calculated, from individual cell volumes. Mikroplanktonic organisms smaller than 15  $\mu\text{m}$  were also counted and measured. Some large representatives of the mikroplankton were enumerated and identified in the entire volume of samples. The data on the taxonomic composition, numbers and biomasses of mikroplanktonic organisms have been prepared during the cruise already.

132 species of microplanktonic organisms were identified in the present material namely 56 dinoflagellate species, 46 diatom species, 20 representatives of other taxonomical groups of flagellated protists, and 10 species of choreotrichous ciliates. Most of diatoms originated from ice ecosystems, whereas the overwhelming majority of flagellates and ciliates represented a typical pelagic assemblage inhabiting ice-free water. The composition of the dinoflagellates was typical for the North Atlantic pelagic ecosystem. Obviously microplanktonic biota are transferred to the Arctic Ocean with prevailing current systems. Here most of warm-water forms die off or transfer into resting stages. Both tend to sink towards deeper regions.

The observed microplanktonic community may be subdivided into two major components representing sufficiently autonomous subsystems of the ecological metabolism which are related to different structural compartments of the water column. The first one, predominated by obligatory autotrophic diatom populations, is related to the ice habitats and its populations seed the topmost layers of the water column. The second one is an assemblage of mixotrophic and heterotrophic microplanktonic organisms inhabiting the water column. The open water parts were dominated by flagellates including the rich and rather diversified dinoflagellate assemblage. The dinoflagellates, together with the smallest fraction of heterotrophic flagellates, formed nearly all of the microplankton biomass.

The irregularities of ice fields create a complicated network of downward fluxes of living, dying off and dead particulate matter. Therefore, the primary production by autotrophic populations of the ice and ice-related communities results in a series of rather short impulses of particulate organic matter in the top layer of the Arctic Ocean.

#### **3.5.4 Epipelagic Community**

31 vertical hauls with a Bongo net were made from 100 m depth to the sea surface, to study the communities of the zooplankton, the size structure of *Calanus sp.* assemblages as well as euphausiids and chaetognaths.

The small copepods (prosome length < 0.5 mm) were abundant at all stations, with the exception of station 057, where the crustaceans from genus *Calanus* were more abundant. Appendicularians and ostracods were the second important taxonomical groups in term of abundance in the deep water area, and appendicularians and chaetognaths in the slope area.

The four assemblages of *Calanus sp.* were distinguished by prosome length structure (Table 5):

- (I) Station 031 - one modal class ( 2.0 - 2.5 mm ).
- (II) Stations 036 - 042 - two modal classes ( 2.5 - 3.0 and 6.0 - 6.5 mm ).
- (III) Stations 044 - 057 - two modal classes ( 3.5 - 4.0 and 6.0 - 6.5 mm )
- (IV) Stations 059 - 062 - one modal class (3.5 - 4.0 mm)

The change of the size structure in *Calanus sp.* assemblages (Table 6) is a reflection of the differences in species and age composition of the assemblages.

**Table 5:** Size structure (%) in the *Calanus* sp. assemblages

Prosoma length, mm	Assemblage I	Assemblage II	Assemblage III	Assemblage IV
1.00-1.50	1.1		1.4	
1.51-2.00	2.2	5.8	1.4	
2.01-2.50	<b>34.0</b>	14.2	5.6	8.3
2.51-3.00	28.6	<b>26.6</b>	9.4	12.5
3.00-3.50	26.4	10.8	17.5	<b>31.2</b>
3.51-4.00	1.1	10.8	<b>34.8</b>	34.4
4.01-4.50	3.3	3.3	6.9	6.2
4.51-5.00		7.5	2.7	2.1
5.01-5.50	1.1	1.1	0.9	1.0
5.51-6.00	1.1	5.0	5.4	2.1
6.01-6.50		<b>8.3</b>	<b>10.0</b>	
6.51-7.00	1.1	5.0	4.0	1.1
7.01-7.50		1.6		1.1
Sum	100.0	100.0	100.0	100.0

Euphausiids were represented by the boreal Atlantic species, *Thysanoessa longicaudata*. The body length of specimens was 12.5 - 20.5 mm and the age was 2 - 4 years. The age structure of euphausiid pseudopopulations can be used to determine the age of the Atlantic water.

Chaetognaths (arrow-worms) are important predators of the marine plankton communities. In the Arctic Ocean four species, *Sagitta elegans*, *S. maxima*, *Eukrohnia hamata* and *E. bathypelagica*. *Sagitta elegans* are dominant in the upper 100 m layer, and three other species reside in bathypelagic levels.

The stages of maturity of *Sagitta elegans* at station 012 are reproduced in Table 6.

**Table 6:** Size structure of *Sagitta elegans* population at station 012

Body length, mm	Stage I	Stage II	Stage III	Stages I-II-III
10.0-15.0	2 (2.0 %)			2 (1.1 %)
15.1-20.0	12 (11.8 %)			12 (6.6 %)
20.1-25.0	28 (27.4 %)	2 (3.1 %)		30 (16.4 %)
25.1-30.0	54 (52.9 %)	22 (32.3 %)	2 (16.6 %)	78 (42.8 %)
30.1-35.0	4 (3.9 %)	38 (55.8 %)	8 (66.6 %)	50 (27.4 %)
35.1-40.0	2 (2.0 %)	6 (8.8 %)	1 (8.4 %)	9 (5.0 %)
40.1-45.1				
45.1-50.0			1 (8.4 %)	1 (0.7 %)
Sum	102	68	12	182

### 3.5.5 Meso- and Bathypelagic Communities

The general pattern of mesozooplankton distribution in the Arctic Ocean is well documented. Vertical changes in abundance, biomass and community structure are mostly a consequence of the marked stratification of the water column. The Polar Surface Water, Atlantic Layer and Polar Deep Water strongly differ in environmental factors and are inhabited by different zooplankton communities. The permanent ice coverage leads to a very short phytoplankton bloom and a low primary production. This results in a short pulsed flux of organic matter into the depth. Therefore the mesopelagic zooplankton community should be well adapted to long starvation periods.

In contrast to the life cycles of intensively studied dominant epipelagic species, e.g. *Calanus* spp., the ecological role and the adaptive strategies of meso- and bathypelagic species in the Arctic are unknown. These organisms are mostly omnivorous or carnivorous and have to rely on living and dead organic material sinking down from the euphotic zone as a food resource.

Because previous investigations have shown that these meso- and bathypelagic communities represent roughly 2/3 of all Arctic zooplankton, they significantly influence the energy flux within the Arctic marine ecosystem. They affect the remineralisation of nutrients within the water column. As predators they have an impact on herbivorous zooplankton populations. Omnivores transform sedimenting organic particles by feeding on detritus and faecal material (coprophagy). In addition, they produce faecal pellets themselves and may modify the transport mechanisms of particular organic carbon. Faecal pellets form a large fraction of the entire sedimenting matter. Due to their properties, i. e. size, density and high energy content, faecal pellets seem to be an important component in the nutrient regime of the deep sea.

During this expedition the feeding ecology of meso- and bathypelagic zooplankton species as well as trophic relationships within the pelagic realm and the impact of this zooplankton community on the particle flux within the water column was studied. Additionally the competition between bathypelagic species was investigated.

Along the cruise track 13 deep Bongo net hauls (mesh sizes 500/300  $\mu\text{m}$ , 300/200 $\mu\text{m}$ ) covering depths down to 2000 m were sampled in the Nansen, Amundsen and Makarov Basins. Individuals of abundant species were sorted out alive and kept in cold containers for later measurements and experiments. Gut evacuation rates (GER) of carnivorous, omnivorous or herbivorous feeding types were measured. The faecal material was collected and preserved for density measurements and LM and SEM investigations. During the following feeding experiments the same individuals were fed with *in situ* algae, faecal pellets from the herbivorous *Calanus glacialis* and undetermined detritus (collected by a small net with 70  $\mu\text{m}$  mesh size attached to the bongo net). Again faecal material was collected and preserved for comparison with *in situ* pellets. The results will allow a qualitative statement on the feeding ecology of the investigated species and will deliver useful values to estimate the role of faecal pellets in the organic particle flux. Measurements of C/N, lipids and carbon isotope ratios will support the understanding of the trophic dynamics in the mesopelagic realm.

The Bongo net samples also provided carnivorous specimens for starvation and feeding experiments on board, as well as for respiration measurements and biochemical analyses. The loss of lipids during starvation will allow to calculate individual energy demands. Respiration measurements offer a second independent opportunity to estimate energetic requirements. Feeding experiments conducted with different carnivorous and prey species elucidated the trophic relationships within the bathypelagic realm.

Additional material was collected by multiple opening/closing net (Multinet) hauls at five stations on the first transect across St. Anna Trough and Voronin Troughs (down to bottom) and at five stations in the Eurasian and Canadian Basins (maximum depth 3600 m). The samples were preserved in 4% formaline and will be analysed in the *Shirshov Institute, Moscow* to confirm the presumed vertical distribution and to complete previous investigations.

The seven investigated mesopelagic copepod species were feeding on algae and faecal pellets, whereas epipelagic herbivorous copepods refused to consume faecal pellets. Detritus in form of marine snow was accepted by one mesopelagic species. Two mesopelagic species were omnivorous with carnivorous tendencies. Comparative studies of *in situ* faecal pellets have shown that freshly produced faecal material of copepods has a roughly uniform shape, but may differ in coloration, optical density and size.

The size of a faecal pellet depends on the size of the animals, the gut fullness and the quantity of food. Colours of pellets may depend on the colour of guts. Since various copepods have a selective feeding behaviour the composition of faecal material is more or less specific for certain species. Density measurements will show, if the physical density of a faecal pellet is correlated to a species and its ontogenetic stages.

The analyses of the net samples showed that carnivorous zooplankton species were abundant throughout the entire area. While hydromedusae, ctenophores and chaetognaths were distributed in patches, carnivorous copepods were present at all stations, inhabiting even the surface layer. The experiments especially focused on *Euchaeta* spp., since this genus dominates the Arctic carnivorous copepods.

4. Station List / Stationsliste							
Station	Cast	Date	Time	Latitude	Longitude	Depth	Activities
1	1	16.07.1996	05:19	68-04.5	12-13.2	185	CTD
2	1	16.07.1996	17:06	69-34.2	15-32.4	1900	2 CTD
3	1	24.07.1996	16:18	81-22.8	64-51.9	243	2 CTD
4	1	24.07.1996	19:10	81-28.9	65-50.5	400	2 CTD
5	1	24.07.1996	23:42	81-27.8	66-51.7	601	2 CTD, ES, MNf
6	1	25.07.1996	06:04	81-21.2	68-20.1	603	2 CTD, O
7	1	25.07.1996	14:33	81-13.4	70-03.6	603	2 CTD, ES, MNf, BNf, O
8	1	25.07.1996	20:50	81-15.7	70-56.8	615	2 CTD
9	1	26.07.1996	03:33	81-17.4	72-01.2	608	2 CTD
10	1	26.07.1996	09:46	81-22.6	72-55.5	598	2 CTD, ADCP, ES, O, 2 MNf
11	1	26.07.1996	19:08	81-23.6	73-18.8	567	2 CTD
12	1	27.07.1996	03:48	81-26.0	73-47.4	536	2 CTDES, O, BNf, ADCP
13	1	27.07.1996	15:37	81-26.1	74-12.9	432	2 CTD
14	1	27.07.1996	18:15	81-25.6	74-24.3	395	2 CTD, BNf
15	1	27.07.1996	21:08	81-25.1	74-33.4	302	2 CTD
16	1	28.07.1996	00:13	81-24.9	74-45.4	210	2 CTD
17	1	28.07.1996	03:33	81-25.1	75-44.9	135	2 CTD
18	1	28.07.1996	14:30	81-27.5	77-27.4	133	2 CTD, ES, O
19	1	29.07.1996	00:18	81-27.3	78-57.3	129	2 CTD
20	1	29.07.1996	05:30	81-27.3	80-25.2	201	CTD
21	1	29.07.1996	20:24	81-51.1	81-51.1	262	CTD, CTD + ADCP, O
22	1	30.07.1996	05:00	81-28.2	82-09.7		ES
23	1	30.07.1996	12:43	81-32.6	82-42.5	303	2 CTD, O
24	1	30.07.1996	17:36	81-42.0	82-08.9	344	2 CTD, ES, 2 MNf, BNf, O
25	1	31.07.1996	07:23	81-57.5	83-54.2	427	CTD, CTD + ADCP, ES, O
26	1	31.07.1996	18:02	81-50.0	85-59.6	381	2 CTD, O
27	1	01.08.1996	01:21	81-50.2	88-32.1	338	2 CTD
28	1	01.08.1996	04:10	81-48.4	89-18.4	203	2 CTD
29	1	01.08.1996	06:53	81-44.8	90-15.2	169	2 CTD, ES, O
30	1	01.08.1996	13:44	81-59.1	90-49.8	306	CTD
31	2	01.08.1996	16:21	82-01.7	90-50.0	497	2 CTD, BNf
32	1	01.08.1996	18:23	82-02.4	91-50.0	734	2 CTD
33	1	01.08.1996	21:21	82-03.8	91-15.5	1006	CTD, CTD + ADCP, BNf
34	1	02.08.1996	02:34	82-05.5	91-30.1	1532	2 CTD
35	1	02.08.1996	08:21	82-11.5	91-54.4	2075	CTD, CTD + ADCP, ES, BNf, O
36	1	02.08.1996	18:11	82-20.0	91-59.8	2636	CTD, BNf
37	1	02.08.1996	23:57	82-31.0	92-17.8	2903	CTD
38	1	03.08.1996	05:39	82-40.4	92-31.3	3086	2 CTD, ES, BNf, O
38	2	03.08.1996	06:18	82-40.5	92-31.0	3086	
39	1	03.08.1996	15:12	82-50.5	92-19.0	3261	CTD, ES
40	1	04.08.1996	01:35	83-11.9	94-02.1	3456	CTD, BNf
41	1	04.08.1996	10:01	83-30.0	96-34.8	3615	2 CTD, ES, 2 MNf, O
41	2	04.08.1996	12:44	83-29.0	96-33.9	3620	
42	1	04.08.1996	23:23	83-49.8	98-23.7	3781	2 CTD, BNf, BNf
43	1	05.08.1996	13:29	84-12.1	100-32.0	3777	2 CTD, ES, O
43	2	05.08.1996	15:15	84-11.4	100-33.8	3780	

44	1	05.08.1996	20:15	84-21.6	101-57.3	3764	2 CTD, Bnf, O
44	2	05.08.1996	21:59	84-21.3	101-58.5	3761	
45	1	06.08.1996	03:47	84-29.0	102-55.7	4016	CTD, CTD + ADCP
46	1	06.08.1996	10:31	84-33.3	103-33.2	4167	2 CTD, ES, Bnf, TU, O
46	2	06.08.1996	12:21	84-33.1	103-36.4	4152	
47	1	06.08.1996	17:47	84-41.7	104-22.1	3817	2 CTD
47	2	06.08.1996	19:47	84-41.7	104-21.3	4013	
48	1	07.08.1996	00:42	84-46.7	105-46.6	3861	2 CTD, CTD + ADCP, Bnf
48	2	07.08.1996	03:05	84-46.7	105-46.9	3863	2 MNf, ES, MNt, O
49	1	07.08.1996	13:20	84-60.0	107-37.7	3896	CTD, TU
50	2	07.08.1996	20:23	85-10.1	109-17.3	4422	2 CTD, Bnf, O
51	1	08.08.1996	03:23	85-17.0	111-35.2	4363	CTD
52	2	08.08.1996	10:40	85-24.3	113-00.6	4424	2 CTD, ES, TU, O
54	1	08.08.1996	20:41	85-45.5	117-28.2	4430	2 CTD, Bnf
54	2	09.08.1996	01:54	85-45.8	117-43.5	4370	
55	1	09.08.1996	07:59	85-52.7	121-14.1	4427	2 CTD, ES, MNt, TU, MNf,
55	2	09.08.1996	13:26	85-51.6	121-27.3	4413	Bnf, O
56	1	09.08.1996	21:25	86-09.6	125-48.8	4384	2 CTD, MNf
56	2	10.08.1996	00:01	86-09.1	125-56.8	4384	
57	1	10.08.1996	05:20	86-17.8	130-37.5	4339	CTD, Bnf
58	1	10.08.1996	09:20	86-24.0	134-01.0	4066	2 CTD, ES, Bnf, O
58	2	10.08.1996	11:27	86-23.5	134-11.4	3989	
59	1	10.08.1996	17:16	86-25.8	136-02.6	3635	CTD, Bnf
60	1	12.08.1996	11:06	86-26.2	138-53.5	3018	CTD, O
61	1	12.08.1996	14:34	86-27.8	140-11.5	2149	CTD, Bnf
62	2	12.08.1996	18:55	86-26.7	141-06.2	1191	CTD, ADCP, O
63	2	13.08.1996	00:08	86-26.7	143-07.5	980	CTD, CTD + ADCP, Bnf
64	2	13.08.1996	05:59	86-25.0	144-29.6	878	CTD, ADCP, ES, TU
65	1	13.08.1996	13:30	86-25.2	146-21.5	1063	CTD, ADCP, Bnf, O
66	1	13.08.1996	20:39	86-21.4	148-07.1	988	CTD, ADCP
67	1	13.08.1996	21:43	86-19.3	150-49.8	1180	CTD, ADCP, Bnf, O
68	1	14.08.1996	02:08	86-14.6	153-01.1	1513	CTD
69	1	14.08.1996	07:47	86-10.3	155-00.3	1340	ES, MNf, Bnf, CTD, O
70	1	14.08.1996	13:10	85-59.5	159-58.4	2217	CTD, O
71	1	14.08.1996	18:25	85-58.0	160-30.6	2907	Bnf, CTD
72	1	14.08.1996	21:26	85-49.7	161-40.9	3923	2 CTD, MNt, 2 MNf, O
72	2	15.08.1996	02:48	85-48.7	161-35.3	3928	
73	1	16.08.1996	07:20	83-01.1	150-16.7	2630	2 CTD, ES, Bnf, MNf, O
73	2	16.08.1996	11:36	83-00.3	150-17.7	2572	
74	1	16.08.1996	17:17	82-49.7	147-41.4	2410	CTD, Bnf
75	1	16.08.1996	23:54	82-39.3	145-27.3	2212	CTD
76	1	17.08.1996	05:40	82-31.5	143-33.6	1958	CTD, ES, MNt, 2 MNf, Bnf,
							Bnf, TU, O
77	1	18.08.1996	04:37	82-30.9	141-13.2	1487	CTD, ADCP
78	1	18.08.1996	13:32	82-30.1	140-03.0	2307	2 CTD, ES, O, ADCP, TU, Bnf
78	3	18.08.1996	16:35	82-30.3	140-04.8	2318	
79	1	18.08.1996	21:00	82-30.0	138-28.3	3599	CTD, ADCP
80	1	19.08.1996	05:09	82-29.8	136-24.8	3854	CTD, ES, O, 2MNf, MNt, Bnf
81	1	19.08.1996	17:55	82-29.9	134-36.3	3891	CTD, ES, Bnf
82	1	20.08.1996	04:50	82-31.3	132-57.2	3857	2 CTD, ES, MNf, TU, O

82	2	20.08.1996	08:08	82-31.5	132-53.8	3972	
83	1	22.08.1996	06:00	81-59.6	131-40.1	295	ES, ADCP
83	1	23.08.1996	02:15	81-57.0	131-39.5		
84	1	23.08.1996	09:36	81-04.4	138-55.3	1757	CTD, MNf, O
85	1	23.08.1996	14:02	81-03.9	138-01.6	2256	CTD, BNf
86	1	23.08.1996	19:49	81-04.5	136-45.3	2750	CTD
87	1	24.08.1996	01:56	81-04.6	135-41.4	3088	2 CTD, BNf
87	2	24.08.1996	03:55	81-05.0	135-41.0	3092	
88	2	24.08.1996	23:27	81-04.6	139-42.8	1539	2 CTD, ADCP, BNf
89	1	25.08.1996	11:54	80-59.2	141-48.1	1697	CTD, ES, BNf, O, ADCP, TU
90	1	26.08.1996	06:12	80-55.4	144-16.3	1846	CTD, ES, TU, MNf, BNt, O
91	1	27.08.1996	11:34	80-31.1	148-35.8	1987	CTD, BNf, O
92	1	27.08.1996	18:25	80-25.8	149-29.2	1931	CTD
93	1	28.08.1996	18:51	80-19.4	150-06.9	1730	CTD, ADCP, O
94	1	29.08.1996	07:32	80-09.2	150-03.7	1299	CTD, ES, ADCP
95	1	29.08.1996	19:15	79-59.8	149-55.7	713	CTD, ADCP, BNf
96	1	30.08.1996	05:14	79-49.4	149-13.2	500	CTD
97	1	30.08.1996	09:44	79-39.5	148-40.5	288	CTD, ES, MNf, BNf, O
98	1	01.09.1996	08:56	78-31.3	133-55.0	1828	CTD, ADCP, O
99	1	01.09.1996	21:27	78-58.0	133-09.0	3004	CTD, 3 BNt
100	1	02.09.1996	09:05	78-49.4	132-48.7	2970	CTD, ES, TU, MNf, BNf, O
101	1	02.09.1996	13:33	78-43.0	132-40.3	2924	CTD, TU
102	1	02.09.1996	23:03	78-33.4	132-13.3	2303	CTD, BNf, ADCP
103	1	03.09.1996	06:16	78-27.1	132-39.9	2202	CTD, ADCP, ES
104	1	03.09.1996	12:20	78-17.6	132-32.5	1906	CTD, BNf, ADCP
105	1	03.09.1996	18:24	78-07.9	132-27.1	1264	CTD, ADCP
106	1	03.09.1996	23:18	78-01.8	132-22.4	548	CTD, ADCP, O
107	1	04.09.1996	02:05	77-59.5	132-30.0	268	CTD
108	1	04.09.1996	10:00	77-41.6	129-45.9		TU
109	1	05.09.1996	05:20	77-27.2	125-08.1		TU, ES
110	1	05.09.1996	12:10	77-26.1	125-24.4		TU

## 5. Participating Institutions / Beteiligte Institutionen

	<i>Acronym</i>	<i>Institution</i>	<i>No. of Participants</i>
<i>Germany</i>	AWI	Alfred-Wegener-Institut für Polar- und Meeresforschung Am Handelshafen 12 27570 Bremerhaven	13
		AERODATA Flugmeßtechnik GmbH Forststr. 33 38108 Braunschweig	1
	DWD	Deutscher Wetterdienst Seewetteramt Postfach 30 11 90 20304 Hamburg	2
	HSW	Helicopter-Service Wasserthal GmbH Kätnerweg 43 22393 Hamburg	4
	IfMH	Institut für Meereskunde der Universität Hamburg Tropowitzstr. 7 22529 Hamburg	2
	IfMK	Institut für Meereskunde der Universität Kiel Düsternbrooker Weg 20 24105 Kiel	2
	IMKH	Institut für Meereskunde und Klimatologie der Universität Hannover Herrenhäuser Str. 2 30419 Hannover	2
	IPÖ	Institut für Polarökologie der Universität Kiel Wischofstr. 1-3, Geb. 12 24148 Kiel	2
	IUH	Institut für Umweltphysik der Universität Heidelberg Im Neuenheimer Feld 366 69120 Heidelberg	1
	<i>Russia</i>	AARI	Arctic and Antarctic Research Institute 38, Ul. Bering 199226 St. Petersburg

	MMBI	Murmansk Marine Biological Institute 17, Vladimirskaia St. Murmansk 183010	2
	OAP	Obuchov Institute of Atmospheric Physics Pyzhevskiy Pereulok 3 109017 Moscow	1
<i>Sweden</i>	GU	Göteborg University Dept. of Oceanography Earth Science Centre 41381 Göteborg Dept. of Analytical and Marine Chemistry 41296 Göteborg	7
<i>Canada</i>	BIO	Bedford Institute of Oceanography P.O. Box 1006 Dartmouth N.S. B2Y 4A2	3
<i>USA</i>	UW	University of Washington, APL 1013 NE 40th Seattle, WA 98105	1
	ESR	Earth & Space Research 1910 Fairview E., no. 102 Seattle, WA 98102-3699	1
	SIO	SCRIPPS Institution of Oceanography University of California, San Diego La Jolla, CA 92093-0214	2
	LDEO	Lamont-Doherty Earth Observatory of Columbia University RT 9W Palisades, New York, 10964-8000	1
<i>Finland</i>	HUT	Helsinki University of Technology Tietotie 1 02150 Espoo	1
<i>U.K.</i>	SPRI	Scott Polar Research Institute University of Cambridge Lensfield Road Cambridge, CB2 1ER	1
<i>Ireland</i>	UCD	University College Dublin Dept. of Experimental Physics Belfield, Dublin 4	1

## 6 Participants / Fahrtteilnehmer

Name	Institution	Nationality
Abrahamsson, Katarina	GU	Swedish
Andersson, Leif	GU	Swedish
Auel, Holger	IPÖ	German
Augstein, Ernst	AWI	German
Bahrenfuß, Kristin	IfMK	German
Björk, Göran	GU	Swedish
Buchner, Jürgen	HSW	German
Bussmann, Ingeborg	AWI	German
Chierici, Melissa	GU	Swedish
Cohrs, Wolfgang	AWI	German
Cottier, Finlo Robert	SPRI	British
Darnall, Clark	U W	USAmerican
Darovskikh, Andrey	AARI	Russian
Drübbisch, Ulrich	IfMH	German
Druzhkov, Nikolay V.	MMBI	Russian
Ekdahl, Anja	GU	Swedish
Ekwurzel, Brenda	LDEO	USAmerican
England, Joachim	DWD	German
Fitznar, Hans-Peter	AWI	German
Frank, Markus	IUH	German
Fransson, Agneta	GU	Swedish
Friedrich, Christine	IPÖ	German
Grachev, Andrey	OAP	Russian
Haas, Christian	AWI	German
Hiller, Scott	SIO	USAmerican
Hingston, Michael Patrick	BIO	Canadian
Hofmann, Michael	IMKH	German
Ivanov, Vladimir	AARI	Russian
Johnsen, Klaus-Peter	AWI	German
Jones, Edward Peter	BIO	Canadian
Larsson, Anne-Marie	GU	Swedish
Lensu, Mikko	HUT	Finnish
Leon Vintro, Luis	UCD	Spanish
Lundström, Volker	HSW	German
Lüpkes, Christof	AWI	German
Muench, Robin	ESR	USAmerican
NN (Ice Pilot)	Murmansk Shipping	Russian
NN (Observer)	Murmansk Shipping	Russian
Pivovarov, Sergey	AARI	Russian
Riewesell, Christian	HSW	German
Rudels, Bert	IfMH	Swedish
Schauer, Ursula	AWI	German
Scherzinger, Till	AWI	German
Schreiber Detlev	HSW	German
Schürmann, Mathias	AERODATA	German
Siebert, Holger	IMKH	German

Sonnabend, Hartmut	DWD	German
Strohscher, Birgit	AWI	German
Templin, Michael	AWI	German
Timmermann, Axel	AWI	German
Timofeev, Sergey	MMBI	Russian
Weissenberger, Jürgen	AWI	German
Wilhelm, Dietmar	IfMK	German
Williams, Bob	SIO	USAmerican
Zemlyak, Frank	BIO	Canadian

## 7. Ship's Crew / Schiffsbesatzung

<u>Profession</u>	<u>Name</u>
01. Captain	Greve, Ernst-Peter
02. 1. Officer	Pahl, Uwe
03. 1. Officer	Rodewald, Martin
04. Chief Engineer	Knoop, Detlef
05. 2 Officer	Grundmann, Uwe
06. 2 Officer	Spielke, Steffen
07. Medical Doctor	Bennemann, J.
08. Radioperator	Koch, Georg
09. 2 Engineer	Erreth, Mon. Gyula
10. 2 Engineer	Ziemann, Olaf
11. 2 Engineer	Fleischer, Martin
12. Electronic Technician	Lembke, Udo
13. Electronic Technician	Muhle, Helmut
14. Electronic Technician	Greitemann-Hackl, A.
15. Electronic Technician	Roschinsky, Jörg
16. Electrician	Muhle, Heiko
17. Boatswain	Clasen, Burkhard
18. Carpenter	Reise, Lutz
19. Sailor	Winkler, Michael
20. Sailor	Bindernagel, Knuth
21. Sailor	Gil Iglesias, Luis
22. Sailor	Pousada Martinez, S.
23. Sailor	Kreis, Reinhard
24. Sailor	Schultz, Ottomar
25. Sailor	Burzan, G.-Ekkehard
26. Sailor	Pulss, Horst
27. Technician	Arias Iglesias, Enrique
28. Technician	Preußner, Jörg
29. Technician	Ipsen, Michael
30. Technician	Husung, Udo
31. Technician	Grafe, Jens
32. Storekeeper	Müller, Klaus
33. Chief Cook	Haubold, Wolfgang

34. Cook	Völske, Thomas
35. Cook	Yavuz, Mustafa
36. 1 Stewardess	Jürgens, Monika
37. Stewardess/Nurse	Dähn, Ulrike
38. Stewardess	Czyborra, Bärbel
39. Stewardess	Deuß, Stefanie
40. Stewardess	Neves, Alexandra
41. 2. Steward	Huang, Wu Mei
42. 2. Steward	Mui, Kee Fung
43. Laundryman	Yu, Kwok Yuen